Clinical Immunology 249 (2023) 109299

Contents lists available at ScienceDirect

Clinical Immunology

journal homepage: www.elsevier.com/locate/yclim

Altered DNA methylation and gene expression predict disease severity in patients with Aicardi-Goutières syndrome

Jessica Garau [a,1], Amandine Charras [b,1], Costanza Varesio [c,d], Simona Orcesi [c,d], Francesca Dragoni [e,f], Jessica Galli [g,h], Elisa Fazzi [g,h], Stella Gagliardi [f], Orietta Pansarasa [i], Cristina Cereda [j,2,3], Christian M. Hedrich [b,k,*,2]

[a] Neurogenetics Research Centre, IRCCS Mondino Foundation, Pavia, Italy
[b] Department of Women's and Children's Health, Institute of Life Course and Medical Sciences, University of Liverpool, Liverpool, United Kingdom
[c] Department of Brain and Behavioral Sciences, University of Pavia, Pavia, Italy
[d] Department of Child Neurology and Psychiatry, IRCCS Mondino Foundation, Pavia, Italy
[e] Department of Biology and Biotechnology, University of Pavia, Pavia, Italy
[f] Molecular Biology and Transcriptomics, IRCCS Mondino Foundation, Pavia, Italy
[g] Department of Clinical and Experimental Sciences, University of Brescia, Brescia, Italy
[h] Unit of Child Neurology and Psychiatry, ASST Spedali Civili of Brescia, Brescia, Italy
[i] Cellular Model and Neuroepigenetics, IRCCS Mondino Foundation, Pavia, Italy
[j] Genomic and post-Genomic Center, IRCCS Mondino Foundation, Pavia, Italy
[k] Department of Paediatric Rheumatology, Alder Hey Children's NHS Foundation Trust Hospital, Liverpool, United Kingdom

ARTICLE INFO

Keywords:
Aicardi-Goutières syndrome
DNA methylation
RNASEH2B
Phenotype
Biomarker
Interferon
ISG

ABSTRACT

Aicardi-Goutières Syndrome (AGS) is a rare neuro-inflammatory disease characterized by increased expression of interferon-stimulated genes (ISGs). Disease-causing mutations are present in genes associated with innate antiviral responses. Disease presentation and severity vary, even between patients with identical mutations from the same family.

This study investigated DNA methylation signatures in PBMCs to understand phenotypic heterogeneity in AGS patients with mutations in *RNASEH2B*. AGS patients presented hypomethylation of ISGs and differential methylation patterns (DMPs) in genes involved in "neutrophil and platelet activation". Patients with "mild" phenotypes exhibited DMPs in genes involved in "DNA damage and repair", whereas patients with "severe" phenotypes had DMPs in "cell fate commitment" and "organ development" associated genes. DMPs in two ISGs (*IFI44L, RSAD2*) associated with increased gene expression in patients with "severe" when compared to "mild" phenotypes.

In conclusion, altered DNA methylation and ISG expression as biomarkers and potential future treatment targets in AGS.

1. Introduction

Aicardi-Goutières Syndrome (AGS) is a rare neuroinflammatory disease. It is typically characterized by early-onset neuroinflammation with cerebrospinal fluid lymphocytosis, white matter lesions, cerebral calcifications, and brain atrophy. Most children affected develop severe disability with motor and cognitive impairment [1]. Notably, AGS shares symptoms with the systemic inflammatory disease Systemic Lupus Erythematosus (SLE) and congenital virus infections, including cutaneous chilblain lesions, increased expression of type I interferons (IFNs) and interferon sensitive genes (ISGs), anaemia, neutropenia and thrombocytopenia [2–4]. Thus, AGS has been classified as a "type I

* Corresponding author at: Department of Women's and Children's Health, Institute of Life Course and Medical Sciences, University of Liverpool, Liverpool, United Kingdom.
E-mail address: chedrich@liverpool.ac.uk (C.M. Hedrich).
[1] These authors share first authorship.
[2] These authors share last authorship.
[3] Present address: Functional Genomic and rare diseases Unit, Department of Pediatrics, Children's Hospital "V. Buzzi", Milan, Italy.

https://doi.org/10.1016/j.clim.2023.109299
Received 19 December 2022; Received in revised form 6 February 2023; Accepted 15 March 2023
Available online 22 March 2023

interferonopathy", a group of Mendelian disorders characterized by mutations in genes involved in type I IFN signalling and innate antiviral responses [5].

Aicardi-Goutières Syndrome is a genetic disorder caused by mutations in (at least) 9 individual genes, namely *TREX1, RNASEH2B, RNASEH2C, RNASEH2A, ADAR1, SAMHD1, IFIH1, LSM11* and *RNU7-1* [6–8], all involved in nucleic acid sensing and/or metabolism [6,7]. The majority of AGS patients carry loss-of-function mutations in *RNASEH2B* (36% worldwide, 59% in Italy) [7,8], encoding for one of the three subunits of RNase H2 enzyme. Within this group, homozygous *RNASEH2B* p.A177T mutations are the most common [7,8]. Notably, mutations in *RNASEH2B* have also been reported in SLE, suggesting shared pathomechanisms between these two diseases [9]. AGS patients carrying p.A177T mutation in *RNASEH2B* show pronounced phenotypic variability, even within the same family [7].

Notably, disease phenotypes of patients with AGS can vary significantly, even between family members who share identical mutations. While some AGS patients present classical "severe" phenotypes characterized by tetraparesis and severe intellectual disability, some patients experience later disease onset and "mild" manifestations. Indeed, some subjects have relatively preserved intellectual function, communication skills and manual abilities [10]. Thus, a neurologic severity score was developed to quantify disease severity from "mild" to "severe" (11), aiming at stratification of patients towards individualized care.

To date, the molecular mechanisms underlying clinical variability of AGS, especially in patients carrying identical mutations, remain unknown [11]. It is tempting to speculate that the degree of cytokine dysregulation and associated inflammation may associate with disease severity, although there is no published evidence in support of this hypothesis. Over recent years, a group of mechanisms determining the accessibility of gene regulatory elements to the transcriptional complex without affecting the underlying DNA sequence has been established and named "epigenetic" events. Alterations to the epigenome, including DNA methylation, have been linked with systemic inflammation in SLE and other systemic inflammatory diseases [12,13]. In some cases, epigenetic alterations even associate with disease activity and severity [14]. To date, only one study investigated epigenetic changes in fibroblasts derived from AGS patient and described reduced DNA methylation in genomic regions that associated with an accumulation of RNA:DNA hybrids [15]. However, altered DNA methylation as a possible modulator of AGS disease severity in individuals sharing the same genotype has not been investigated yet. To explore the hypothesis that DNA methylation influences gene expression, thereby affecting associated clinical phenotypes in AGS patients with the same mutation (*RNASEH2B* p.A177T), we performed genome-wide DNA methylation profiling in peripheral blood mononuclear cells (PBMCs) from AGS patients and healthy controls.

2. Materials and methods

2.1. Patients and controls

For DNA methylation analysis, ten AGS patients and six healthy controls were recruited for this study. Patients with AGS were enrolled at the IRCCS Mondino Foundation, Pavia, Italy. All patients carried the p.A177T mutation in *RNASEH2B* and were diagnosed with a "mild" ($N = 5$) or "severe" ($N = 5$) AGS phenotype based on a composite score combining the Gross Motor Function Classification System [16], the Manual Ability Classification System [17], and the Communication Function Classification System [18]. The resulting composite functional severity score ranged from three (fully preserved motor and communicative function) to 15 (extremely severe impairment of motor and communicative function). A score ≥ 12 denoted severe impairment, a score < 12 mild impairment. Since the composite functional score is not able to sufficiently differentiate individuals at the lower end of function [11], to better define clinical severity of AGS symptoms and to avoid as much as possible a relevant "floor effect", a recently developed multimodal tool for the assessment of neurologic function in AGS [11] was retrospectively applied to each patient. This final AGS scale score ranges from 0 (no neurodevelopmental acquisition) to 11 (preserved neurological function). We chose a score focusing on neurological symptoms in the absence of systemic features (such as chilblains or malar rash, etc.) because we aimed to define molecular signatures that correlate with neurological outcomes to work towards predictive biomarkers that may be used for patient stratification and individualized care. We feel this is of key importance, as neurological outcomes are currently not predictable, while chilblains and skin rashes can be managed when present.

Ethnicity and sex matched healthy volunteers were enrolled at the Transfusion Centre of the IRCCS Policlinico S. Matteo Foundation in Pavia, Italy (Supplementary Table 1). To validate interferon mRNA expression signatures, 18 AGS patients carrying mutations in *RNASEH2B, RNASEH2C, ADAR1, SAMHD1*, or *IFIH1* and 10 healthy controls were recruited (Supplementary Table 2).

2.2. Ethics

The study was approved by the local ethics committee (approval n. 3549/2009 of 30/9/2009 and 11/12/2009, and n.20170035275 of 23/10/2017), IRCCS Mondino Foundation, Pavia, Italy. Written informed consent was obtained from all participants and/or their legal guardians.

2.3. Sample processing and DNA isolation

PBMCs were isolated from EDTA blood using standard ficoll (Sigma Aldrich, MO, USA) gradient centrifugation. Genomic DNA was extracted using a semi-automated method: Maxwell® 16 System DNA Purification (Promega, Madison, WI, USA). DNA was quantified with NanoDrop ND1000 UV–Vis Spectrophotometer and Qubit® fluorometer (Thermo Scientific, Waltham, MA, USA).

2.4. Genome-wide methylation profiling

The DNA methylation status if >850,000 CpGs was assessed using the Illumina Infinium MethylationEPIC array BeadChip (850 K) (Diagenode Epigenomic Services, Vienna, Austria, Cat No. G02090000). Samples from healthy controls and AGS patients with "mild" and "severe" disease phenotypes were randomly distributed across assays to avoid bias through batch effects.

DNA methylation data were analyzed using the *Minfi* and *ChAMP* packages for R [19,20]. Data acquisition, pre-processing, quality control and normalization of methylation data were performed as described previously [13]. Batch effects and covariates ("age category" and "gender") were identified and corrected using the *ComBat* function of the *ChAMP* package [21].

For downstream analysis and data visualization, numerical Beta (β) values were generated ranging from 0 (0% methylation) to 1 (100% methylation). Differentially methylated positions (DMPs) were determined based on M values (logit transformation of β) using empirical Bayes' moderated *t*-test method, contained in the *limma* R package [22]. False discovery rates (FDR) <0.05 were used as significance thresholds. Only probes with a difference in β values over 10% were kept for analysis ($|\Delta\beta| > 0.1$). Differentially methylated regions (DMRs) were identified using the DMRCate package [23]. DMPs and DMRs identified were annotated with relevant information about location of probes such as their genomic position, gene annotation, etc. The limma pipeline was used for differential methylation analysis and to calculate moderated t-statistics; the dmrcate() function was used to combine CpGs to extract DMRs with a β value cut-off of 10% and a minimum of 15 CpGs.

2.5. Pathway prediction analysis

Gene enrichment analysis was performed for genes presenting at

least one promoter DMP (TSS1500, TSS200, 5′UTR). Gene Ontology (GO) analysis for biological processes, cellular components and molecular functions, and KEGG pathway analysis (Kyoto Encyclopedia of Genes and Genomes) were performed using the R package *clusterProfiler* [24]. Only significant GO terms and KEGG pathways were included in this report (Bonferroni corrected, $p < 0.01$). To display results, identified pathways and terms were ordered according to adjusted p values; complete lists including all KEGG pathways and GO terms identified are reported in the Supplementary Tables.

2.6. Interferon score

Peripheral blood from AGS patients carrying the *RNASEH2B* p.A177T mutation and "mild" ($N = 5$) or "severe" ($N = 5$) phenotypes and 11 healthy controls was collected (PaxGene™ tubes, PreAnalytiX, Hombrechtikon, Switzerland). Tubes were kept at room temperature for 2 h and frozen at −80°C. RNA extraction was performed following manufacturer's instructions (PAXgene Blood RNA Kit, PreAnalytiX, Hombrechtikon, Switzerland). RNA concentrations were measured using the NanoDrop ND1000 UV–Vis Spectrophotometer (Thermo Scientific, Waltham, MA, USA). Reverse transcription into cDNA was performed using 800 ng of RNA and the iScript™ Reverse Transcription Supermix kit for RT-qPCR (Bio-Rad, Hercules, CA, USA). Gene expression was measured using the TaqMan Universal PCR Master Mix (Applied Biosystems, Paisley, UK) and the Bio-Rad CFX96™ qPCR platform. The relative abundance of target transcripts was measured using TaqMan probes for *IFI44L* (Hs00199115_m1), *RSAD2* (Hs01057264_m1), *IFI27* (Hs01086370_m1), *IFIT1* (Hs00356631_g1), *ISG15* (Hs00192713_m1) and *SIGLEC1* (Hs00988063_m1), and *HPRT1* (Hs03929096_g1). Gene expression levels in AGS patients were normalized to the average expression in 11 healthy controls. As previously suggested by Rice et al. [25], median fold changes of two ISGs compared to *HPRT1* housekeeping gene in 10 normal controls plus two SDs (+2 SD) was used to create an interferon score (Here: 2.46). For each patient, the normalized fold change relative to mean values in healthy controls was calculated. The interferon score consists of the geometric mean of the two genes included (*IFIH1* and *RSAD2*); it was considered "positive" when above the score in healthy controls (>2.46).

2.7. Gene expression

To quantity gene expression of differentially methylated genes *ATM, LIG4, SMG6, RAD50, TERF2, RAB34, SH2D1B* and *ADAMTS9*, standard semi-quantitative SYBR Green assays, using 200 nM of each oligonucleotide, 5 μL of SYBR Green SuperMix (BioRad, Richmond, CA, USA), and 1 μL of cDNA template or water control. Primer sequences are available upon reasonable request. Mean Ct values were normalized against those determined for the *HPRT1* housekeeping gene. Fold-change differences relative to healthy controls were determined using the $2^{-\Delta\Delta Ct}$ method [26].

2.8. Calculation of IFN methylation scores

The Interferome database V.2.01 (http://www.interferome.org) was used for the identification type 1 IFN-regulated genes in our set of genes for which DMPs had been identified [27]. Methylation scores were calculated as previously suggested by Björk et al. [28]. Briefly, means ($Mean_{HC}$) and standard deviation (SD_{HC}) for each DMP associated to type 1 IFN-regulated genes in the healthy control group were used to achieve standardised values (SVs) for each individual according to the formula: $SV = (Value\text{-}Mean_{HC})/SD_{HC}$, SVs were summed up to total scores [28].

2.9. Statistical analysis

Geometrical means and standard deviations were used to display data. One-Way Analysis of Variance (ANOVA) was used for statistical analysis, followed by the post hoc Tukey's test (GraphPad Prism version 5, USA). Shapiro–Wilk normality tests were performed to assess Gaussian distribution before testing statistical associations between two variables using Pearson's correlation. P-values <0.05 were considered statistically significant. Where appropriate, for multiple comparisons, *Bonferroni* adjustment was used and $p < 0.01$ was considered significant.

3. Results

3.1. Clinical characterization

Ten AGS patients with the p.A177T mutation in *RNASEH2B* were enrolled in the study (Table 1). Five patients presented with the classical "severe" phenotype with spastic-dystonic tetraparesis, severely impaired fine-motor and communication abilities. The remaining five patients presented with a "mild" phenotype, characterized by spastic diplegia in two cases, and hemiparesis in two cases. Spastic-dystonic tetraparesis was present in one of these patients. In all patients with "mild" phenotype, fine motor function is preserved with the ability of handling objects, and communication function is preserved or quite adequately represented in all patients.

3.2. DNA methylation patterns vary between AGS patients and controls

Comparing DNA methylation profiles of all AGS patients with mutations in *RNASEH2B* to healthy controls, we identified 31,598 DMPs uniquely associated with 10,052 genes (Fig. 1A). Investigating the distribution of DMPs in relation to CpG island, the vast majority were in the "open sea" (70.63%). When considering their location in relation to genes, a high percentage of DMPs was in promoters (52.52%, of which 27.73% were in 5′ untranslated regions (UTRs), 8.33% in the TSS200 and 16.46% in the TSS1500), followed by intergenic regions (21.38%) and 3' UTRs (20.87%) (Fig. 1B).

To link altered DNA methylation with signalling pathways, GO terms enrichment and KEGG pathway analysis were performed. Because DNA methylation in promoters correlates with low/no transcriptional activity [29], we focused on 27,202 promoter DMPs (17,951 hyper-, 9251 hypomethylated) uniquely associated with 8807 genes. KEGG analysis of differentially methylated promoters revealed the involvement of "Platelet activation" ($p = 2.65 \times 10^{-8}$), "Chemokine signalling pathway" ($p = 1.62 \times 10^{-6}$) and "Endocytosis" ($p = 2.95 \times 10^{-5}$) in AGS (Fig. 1C and Supplementary Table 3). GO analysis of "Biological Processes" delivered associations between AGS and "mononuclear cell differentiation" ($p = 3.20 \times 10^{-14}$) and "lymphocyte differentiation" ($p = 3.02 \times 10^{-13}$). "Cellular Components" analysis delivered genes involved in "focal adhesion" ($p = 6.45 \times 10^{-18}$) and "cell-substrate junction" ($p = 6.27 \times 10^{-17}$). GO "Molecular Functions" analysis delivered enrichment of "GTPase regulatory activity" (both $p = 8.28 \times 10^{-15}$) and "actin binding" ($p = 1.24 \times 10^{-13}$) in AGS (Fig. 1D and Supplementary Table 4).

3.3. Differentially methylated positions shared between "mild" and "severe" AGS patients

Next, we sought to identify DMPs that were shared between AGS patients with "mild" and "severe" phenotypes but not with healthy controls, and such that were distinctly associated with AGS phenotypes ("mild" vs "severe"). A total of 11,244 DMPs (in the promoters of 6822 genes) were shared between "mild" and "severe" AGS phenotypes: 9175 DMPs (in 3178 genes) uniquely associated with "mild" and 1003 DMPs (associated with 522 genes) uniquely associated with "severe" AGS phenotypes (Supplementary Fig. 1).

Gene enrichment analysis considering differentially methylated genes that were shared between "mild" and "severe" AGS phenotypes revealed identical results to above mentioned KEGG analyses, including

Table 1
Clinical features of AGS patients with RNASEH2B p.A177T mutations and "mild" or "severe" phenotypes.

Phenotype	Age at sample collection	Disease onset	Neurological phenotype	Gross Motor Function	Manual Ability	Communication Function	Composite score	AGS score
"Mild"								
Pt 1	3y	late	hemiplegia	II – walks with limitations	I – handles objects easily and successfully	I – effective sender and receiver with unfamiliar and familiar partners	4	11
Pt 2	1y	late	spastic-dystonic tetraparesis	V – transported in a manual wheelchair	III – handles objects with difficulty	III – effective sender and receiver with familiar partners	11	6
Pt 3	3y	neonatal	hemiplegia	II – walks with limitations	I – handles objects easily and successfully	I – effective sender and receiver	4	11
Pt 4	6y	late	spastic diplegia	III – walks using a held-mobility device	II – handles most objects, but with somewhat reduced quality	I – effective sender and receiver	6	10
Pt 5	5y	infantile	spastic diplegia	II – walks with limitations	I – handles objects easily and successfully	I – effective sender and receiver	4	10
"Severe"								
Pt 6	5y	infantile	spastic-dystonic tetraparesis	V – transported in a manual wheelchair	V – does not handle objects	V – seldom effective, even with familial partners	15	1
Pt 7	1y	infantile	spastic-dystonic tetraparesis	V – transported in a manual wheelchair	V – does not handle objects	V – seldom effective, even with familial partners	15	2
Pt 8	4y	infantile	spastic-dystonic tetraparesis	V – transported in a manual wheelchair	V – does not handle objects	V – seldom effective, even with familial partners	15	1
Pt 9	3y	infantile	spastic-dystonic tetraparesis	V – transported in a manual wheelchair	V – does not handle objects	V – seldom effective, even with familial partners	15	2
Pt 10	4y	infantile	spastic-dystonic tetraparesis	V – transported in a manual wheelchair	IV – handles a limited selection of easily managed objects in adapted situation	IV – inconsistent with familial partners	13	5

"platelet activation" ($p = 1.05 \times 10^{-6}$), "chemokine signaling pathway" ($p = 3.59 \times 10^{-5}$), "adrenergic signalling in cardiomyocytes" ($p = 2.06 \times 10^{-4}$) and "Th17 cell differentiation" ($p = 3.87 \times 10^{-4}$) (Supplementary Fig. 2A and Supplementary Table 5). GO "Biological Processes" identified included "mononuclear cell differentiation" ($p = 5.73 \times 10^{-11}$), "regulation of small GTPase mediated signaling" ($p = 6.32 \times 10^{-11}$) and "positive regulation of cytokine production" ($p = 7.95 \times 10^{-11}$); GO terms for "Cellular Components" included "focal adhesion" ($p = 7.82 \times 10^{-17}$), "cell-substrate junction" ($p = 4.14 \times 10^{-16}$) and "specific granule" ($p = 2.93 \times 10^{-13}$). Terms for GO "Molecular Functions" included "GTPase regulatory activity" ($p = 9.66 \times 10^{-15}$), "nucleoside-triphosphatase regulator activity" ($p = 9.66 \times 10^{-15}$) and "guanyl-nucleotide exchange factor activity" ($p = 4.17 \times 10^{-12}$), which were also observed above (Supplementary Fig. 2B and Supplementary Table 6).

Notably, several genes previously associated with type I interferon signalling were differentially methylated between AGS patients and controls, which included *IFI44L*, *RSAD2*, *MX1*, *PARP9*, *IFITM1*, *IRF7, IFIT3* and *ADAR1*, one of the 9 AGS-causing genes (Supplementary Fig. 2C) (7).

3.4. Differentially methylated positions separate "mild" from "severe" AGS patients

A total of 9175 promoter DMPs (3004 hypo-, 6171 hypermethylated) uniquely associated with a "mild" AGS phenotype. KEGG analysis considering genes with DMPs associated with "mild" phenotypes identified an enrichment for several immunological pathways, including chemokine ($p = 1.06 \times 10^{-6}$), TNF ($p = 4.55 \times 10^{-4}$) and NF-kB signalling pathways ($p = 6.15 \times 10^{-4}$), T ($p = 7.86 \times 10^{-5}$) and B cell receptor signalling pathways ($p = 9.86 \times 10^{-4}$; Fig. 2A and Supplementary Table 7). GO analysis revealed a significant enrichment of genes involved in "Biological Processes" including "leukocyte activation involved in immune response" ($p = 4.09 \times 10^{-13}$), "cell activation involved in immune response" ($p = 5.38 \times 10^{-13}$) and "mononuclear cell differentiation" ($p = 1.07 \times 10^{-16}$). With respect to "Cellular Components", significantly enriched GO terms included "cell-substrate junction" ($p = 8.04 \times 10^{-13}$) and "focal adhesion" ($p = 1.12 \times 10^{-12}$). GO "Molecular Functions" included "GTPase regulator activity" ($p = 1.45 \times 10^{-12}$), "nucleoside-triphosphatase regulator activity" ($p = 1.45 \times 10^{-12}$) and "actin binding" ($p = 2.55 \times 10^{-11}$) (Fig. 2B and Supplementary Table 8).

Notably, among the most differentially methylated genes associated with "mild" AGS, we observed genes involved in DNA damage and repair (such as *ATM, RAD50*, and *LIG4*), nonsense-mediated mRNA decay (NMD) (*SMG6*) and telomere maintenance (*TERF2*) (Fig. 2C). Semi-quantitative analysis of gene expression levels in PBMCs delivered significant differences between controls and AGS patients with "mild" phenotypes for *TERF2* and *SMG6*. While higher levels of *ATM* and a decreased expression of *LIG4* and *RAD50* were seen in AGS patients with "mild" phenotypes, differences did not reach statistical significance (Supplementary Fig. 3A).

Lastly, we performed a KEGG analysis considering 1003 promoter DMPs (610 hypo-, 393 hypermethylated) uniquely associated with "severe" phenotypes. Enrichment was only noted for one pathway, "Maturity onset diabetes of the young" ($p = 2.46 \times 10^{-3}$) (Fig. 2D and Supplementary Table 9). GO "Biological Processes" enriched terms included "neuron projection guidance" ($p = 2.04 \times 10^{-4}$), "axonogenesis" ($p = 2.22 \times 10^{-4}$) and "axon development" ($p = 2.34 \times 10^{-4}$). We identified one cellular components term associated with "severe" AGS, namely "cell leading edge" ($p = 8.54 \times 10^{-3}$), and three terms for molecular function, all related to DNA-binding transcription activator activity, RNA polymerase II-specific ($p = 1.09 \times 10^{-7}$), DNA-binding transcription activator activity ($p = 1.48 \times 10^{-7}$) and DNA-binding transcription repressor activity ($p = 5.45 \times 10^{-3}$) (Fig. 2E and Supplementary Table 10).

Interestingly, some ISGs (e.g., *IFI44L* and *RSAD2*) exhibited CpGs specifically hypomethylated only in patients with "severe" AGS phenotypes. Moreover, in "severe" AGS patients, genes involved in the "fusion of phagosomes with lysosomes" (*RAB34*), in the "transport from the endoplasmic reticulum to the Golgi" (*ADAMTS9*) and in the "functionality of natural killer (NK) cells" (*SH2D1B*) pathways were found to be

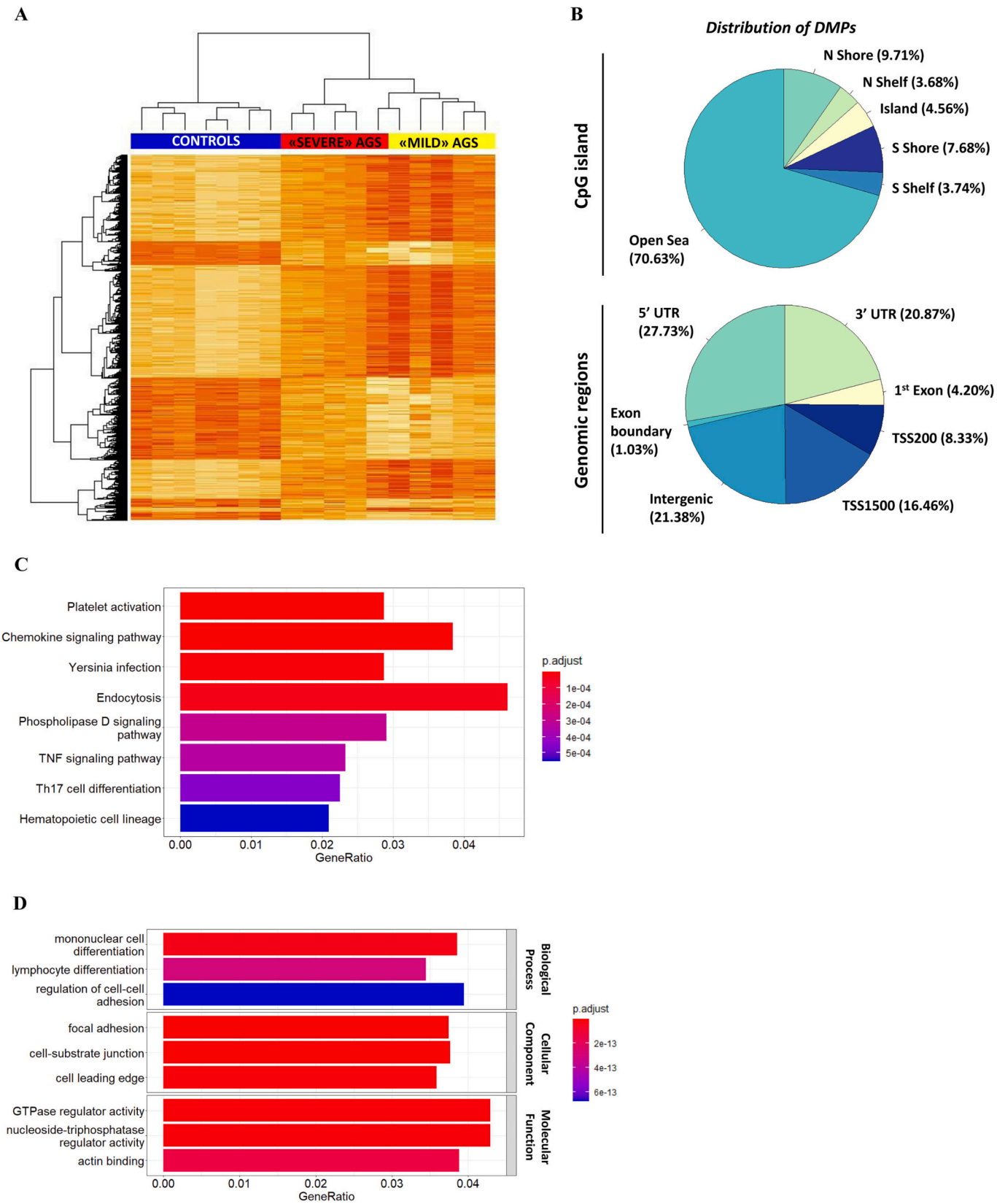

Fig. 1. DNA methylation profiles differentiate PBMCs from AGS patients and healthy controls. (A) Heat map depicting differentially methylated positions (DMPs) between AGS patients carrying the *RNASEH2B* p.A177T mutation and healthy controls (FDR < 0.05, $|\Delta\beta| > 0.1$). Normalized DNA methylation levels are displayed on the right with red indicating reduced methylation and yellow indicating increased methylation levels. (B) Genomic distribution of DMPs in relation to genomic regions and CpG island, respectively. (C) KEGG pathway analysis of genes with at least one DMP in their promoter. (D) GO analysis of differentially methylated genes. GO terms related to biological process, cellular component and molecular function are shown. (For interpretation of the references to colour in this figure legend, the reader is referred to the web version of this article.)

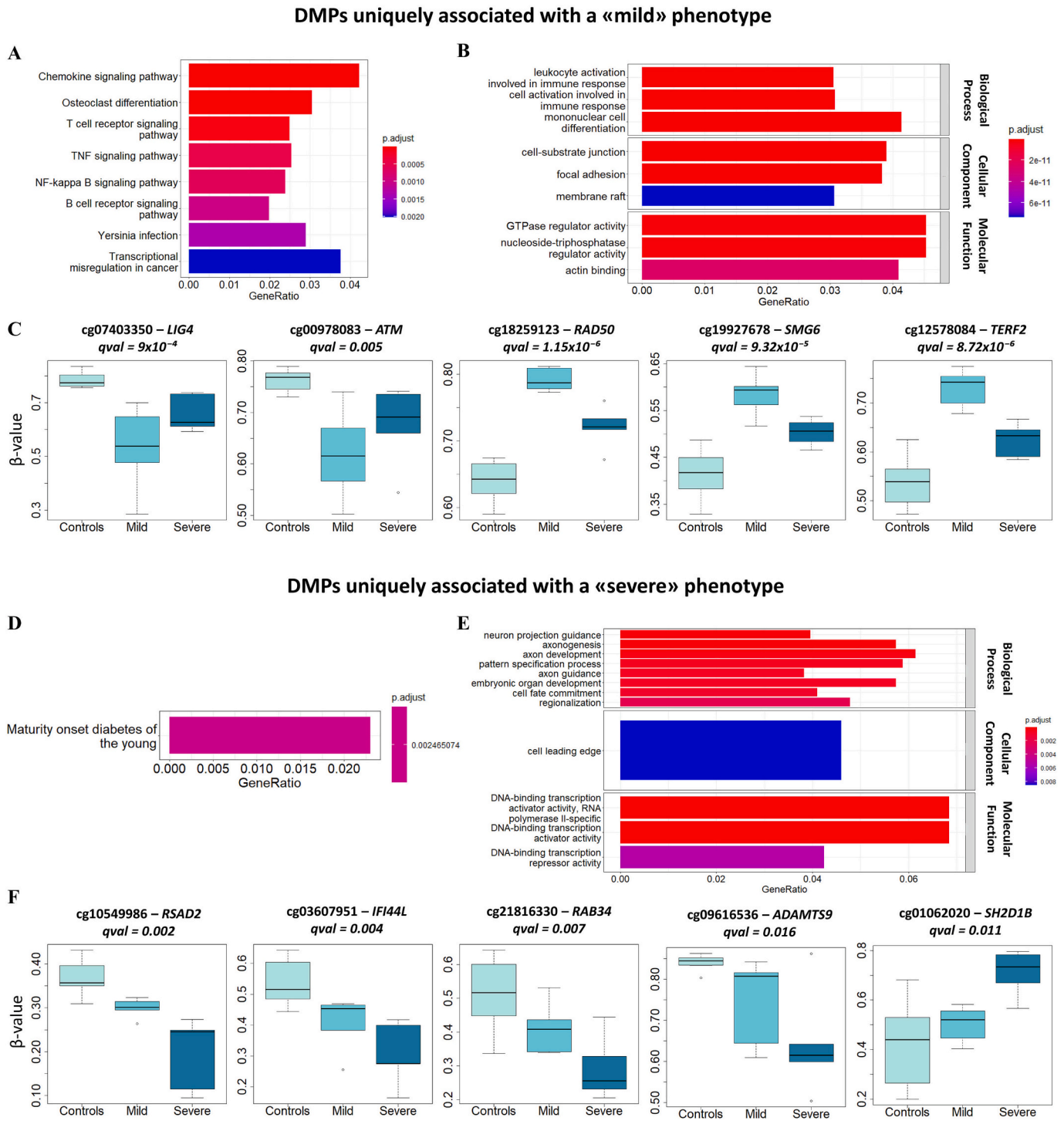

Fig. 2. KEGG and GO analyses of differentially methylated genes uniquely associated with "mild" or "severe" AGS (*RNASEH2B* p.A177T). (A, B) KEGG and GO analyses of genes that were differentially methylated only in AGS patients with "mild" phenotypes. (C) Differences in β values of selected CpG sites identified as DMPs uniquely associated with a "mild" phenotype. (D, E) KEGG and GO analyses of genes that were differentially methylated only in AGS patients with "severe" phenotypes. (F) Differences in β values of selected CpG sites identified as DMPs uniquely associated with a "severe" phenotype.

differentially methylated (Fig. 2F). Expression of *IFI44L* and *RSAD2* was significantly increased in AGS patients with "severe" but not in "mild" phenotypes (Supplementary Fig. 4). Expression of *RAB34* was increased in both "mild" and "severe" AGS. No statistically significant differences were observed for *SH2D1B* (Supplementary Fig. 3B). Notably, *ADAMTS9* was not expressed in ex vivo isolated PBMCs from controls or AGS patients.

3.5. Differentially methylated regions associate with disease severity

To identify larger DMRs associated with AGS and disease phenotypes, regions including a minimum of 15 CpGs were analyzed. As above for DMPs, regions that were shared or uniquely associated with "mild" or "severe" AGS phenotypes were investigated. The majority of DMRs identified (11) were specifically associated with a "severe" disease, 4 associated with AGS but were shared between "mild" and "severe"

disease, and 6 regions were uniquely associated with "mild" phenotypes (Fig. 3A). The 4 DMRs associated with all AGS phenotypes uniquely associated with 10 genes, including the ones encoding for the transcription factors *HIVEP3*, the trans-membrane protein Semaphorin 6B (*SEMA6B*), the acute phase protein Leucine Rich Alpha-2-Glycoprotein 1 (*LRG1*), and the enzymes histidine ammonia-lyase (*HAL*) (Table 2). Genes associated with DMRs are involved in the KEGG pathway "Histidine metabolism" ($p = 0.0107$) (Fig. 3B and Supplementary Table 11). GO "Molecular Functions" analysis highlighted the involvement of "carbon-nitrogen lyase activity" ($p = 0.0226$), "Semaphorin receptor binding" ($p = 0.0399$), "transforming growth factor beta receptor" ($p = 0.0416$), and "chemorepellent activity" ($p = 0.0485$) in both "mild" and "severe" AGS (Fig. 3C and Supplementary Table 12).

Patients with AGS exhibited 6 DMRs uniquely associated with "mild" phenotypes that affect 10 genes including two ISGs, namely *IFITM1* and *IFITM2* (Table 3). Gene enrichment analysis considering genes associated with DMRs delivered enrichment of GO "Biological Processes" "response to interferon-alpha" ($p = 0.0027$), "negative regulation of viral entry into host cell" ($p = 0.034$), "negative regulation of viral life cycle" ($p = 0.048$) and "response to interferon-beta" ($p = 0.073$) (Fig. 3D and Supplementary Table 13). Eleven DMRs specifically associated with "severe" AGS phenotypes affected 17 genes (Table 4), including Integrin Subunit Alpha E (*ITGAE),* Neutrophil elastase *(ELANE),* Ras Homolog Family Member H *(RHOH)* and G Protein-Coupled Receptor Kinase 2 (*ADRBK1),* all involved in immunological pathways and/or neurodevelopment.

3.6. Expression of ISGs correlates with AGS disease severity

Because type I "interferon signature", a routinely performed laboratory test to quantify pathologically activated gene expression and disease activity, are elevated in patients AGS [25], we tested IFN expression to discriminate between "mild" and "severe" AGS phenotypes. Indeed, individual genes included in the signature previously suggested by Rice et al. [8,25] (*IFI44L, IFI27, SIGLEC1*, and *RSAD2*) and the complete signature consisting of 6 genes (also including *IFIT1* and *IST15*) discriminated between "mild" and a "severe" AGS phenotypes (Supplementary Fig. 4). As described above, two ISGs, *IFI44L* and *RSAD2,* were among the most strongly hypomethylated genes in AGS. Considering the expression of abovementioned genes involved in the type I interferon signature, most significant differences were observed in *IFI44L* and *RSAD2* (Supplementary Fig. 4 and Fig. 4A and B). Calculation of a "reduced" interferon score including only *IFI44L* and *RSAD2* using the formula provided by Rice et al. [25], highlighted that almost all patients with "severe" AGS presented a positive interferon score, while only few AGS patients with "mild" phenotypes did (Fig. 4C). Thus, the "reduced" IFN signature may represent a faster and cheaper method to discriminate between these two phenotypes when compared to the "entire" panel of 6 genes.

Lastly, we investigated possible correlations between AGS disease severity and IFN scores considering 10 healthy controls and 10 AGS patients with the *RNASEH2B* p.A177T mutation (5 "mild", 5 "severe" phenotypes), which resulted in the identification of a moderate negative correlation between disease activity and interferon scores ($r = -0.54$, $p = 0.02$) (Fig. 4D). Interferon scores were assessed also in AGS patients carrying mutations in other AGS-related genes, namely *TREX1, RNASEH2C, SAMHD1,* and *IFIH1*. This confirmed the moderate negative correlation between disease severity and ISG expression ($r = -0.57$, $p = 0.002$; Fig. 4E).

3.7. ISG methylation correlates with clinical severity scores

We wondered whether IFN expression is reflected by DNA methylation patterns and calculated an IFN methylation score following the method suggested by Björk et al. [28]. Type 1 IFN-regulated gene associated DMPs were identified using the Interferome database (http://www.interferome.org) [27]. A total of 6421 IFN-associated DMPs were identified relating to 2647 genes (of 9050 genes identified comparing AGS patients versus healthy control; 29% of all genes). IFN methylation scores were higher in AGS patients when compared to healthy controls, and higher in patients with "mild" when compared to "severe" AGS (Fig. 4F). Notably, as DNA methylation can vary in either direction and a large number of genes are included in the score, this does not automatically translate to reduced DNA methylation in one versus the other disease phenotype. Considering DMP-based ISG methylation scores, a positive correlation was identified between methylation scores and AGS disease activity ($r = 0.73$, $p = 0.01$, Fig. 4G). Similarly, when considering DMPs in promoter regions of *IFI44L* and *RSAD2* genes, the methylation score was reduced in AGS patients when compared to controls, no significant differences were observed between "mild" and "severe" phenotypes and no correlation was observed between methylation scores and AGS disease activity (Supplementary Fig. 5).

4. Discussion

This study identified differential DNA methylation and ISG expression patterns in AGS patients carrying the *RNASEH2B* p.A177T mutation when compared to healthy controls, and between AGS patients with "mild" versus "severe" phenotypes. Prediction of developmental trajectories in AGS patients remains challenging and limits the ability to offer individualized care. Indeed, AGS patients show various degrees of neurologic impairment, which particularly applies to patients carrying the "common" p.A117T mutation in *RNASEH2B* [10]. While associations between genotypes and clinical severity exist [7], the molecular causes of variability within individual genotypes have not been revealed.

Molecular modifiers affecting disease phenotypes in monogenic autoimmune/inflammatory diseases are complex and may include genetic factors (e.g., additional risk alleles) and epigenetic alterations [12,30]. The latter may be the result of environmental impacts, hormones, ongoing inflammation [31], and others [32,33]. To date, the molecular mechanisms underlying clinical variability in AGS remain unknown. To investigate the involvement of epigenetic alterations in phenotype variability among AGS patients with the *RNASEH2B* p.A177T mutation, we performed DNA methylation profiling in PBMCs from healthy controls and AGS patients covering a range of clinical phenotypes (from "mild" to "severe"). DNA methylation was chosen as an established epigenetic modification that has been linked with disease expression in individuals predisposed for the development of SLE [34]. Moreover, DNA methylation is considered the most stable epigenetic modification [35]. Comparative DNA methylation profiling of AGS versus controls and "mild" versus "severe" AGS highlighted the involvement of pathways previously associated with autoimmune/inflammatory diseases, including "platelet activation" [36] [37] [38] and "focal adhesion" [39].

Consistent with the increased ISG expression previously reported in AGS [25,40], this study identified altered DNA methylation, which was in agreement with previous studies in clinically related diseases SLE and Sjögren's syndrome [41–45]. Interferon signatures are commonly tested in AGS to assess disease activity and/or severity [46]. To date, no associations between ISG expression and severity have been identified [7,8]. Here, we confirm previously reported increased type I IFN signatures in AGS [25] and, for the first time, identified differential ISG expression between AGS patients with "mild" versus "severe" phenotypes, and "moderate" correlation ($r = -0.54$) [47] between ISG expression and a numeric neurological disease activity score [11]. Notably, differences between controls and disease phenotypes were more pronounced at the DNA methylation level, and correlations between DNA methylation and neurological disease activity was "strong" [47] ($r = 0.73$). Thus, results from this study support a link between altered ISG methylation and AGS phenotypes.

Intriguingly, hypomethylation of *ADAR1*, for which loss-of-function

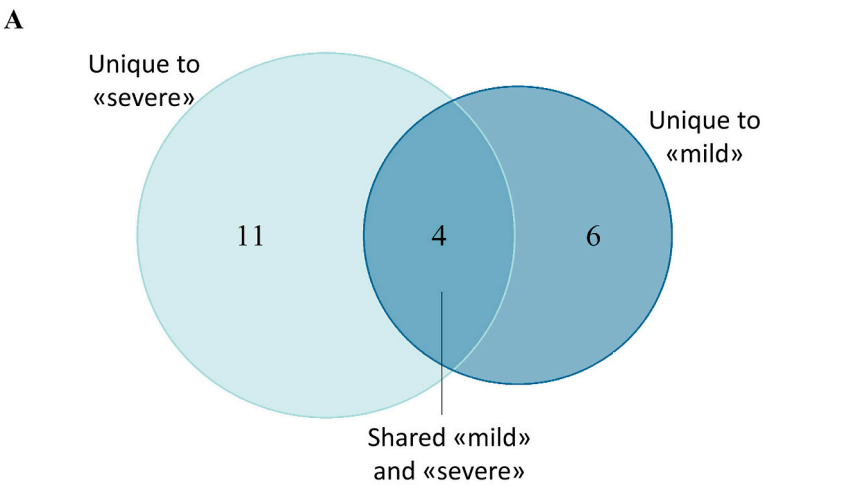

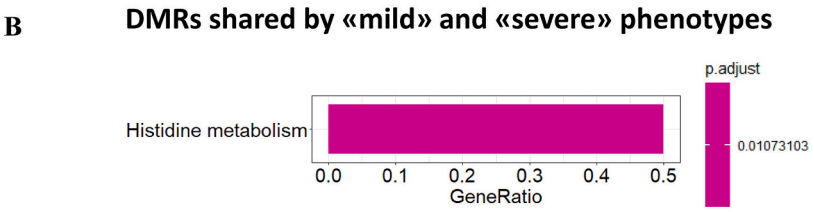

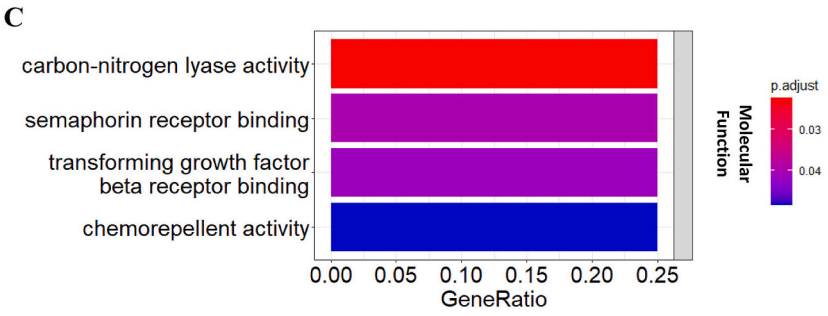

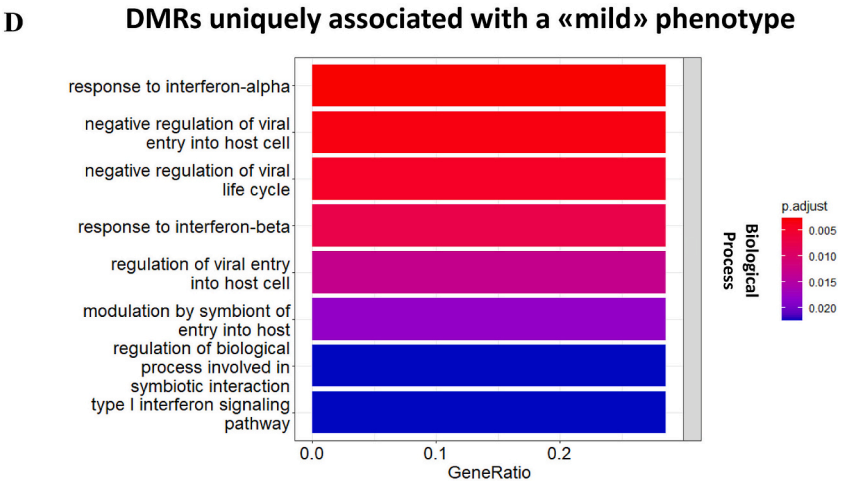

Fig. 3. Shared and phenotype-specific DMRs. (A) A total of 4 DMRs (blue) were shared between "mild" and "severe" AGS phenotypes (*RNASEH2B* p.A177T), 11 DMRs were uniquely associated with a "severe" phenotype (dark blue), and 6 were uniquely associated with "severe" phenotypes (light blue). (B, C) KEGG and GO analyses of genes affected by DMRs and shared by "mild" and "severe" AGS patients. (D) GO analysis of genes affected by DMRs specifically associated with "mild" phenotypes. (For interpretation of the references to colour in this figure legend, the reader is referred to the web version of this article.)

Table 2
DMRs shared between "mild" and "severe" AGS phenotypes.

Chromosome	Start	End	width	strand	Number of CpGs	maxdiff	meandiff	Genes included in the DMR
chr12	96,388,589	96,391,252	2664	*	16	−0.26	−0.11	*RP11-256L6.3, HAL*
chr19	4,539,943	4,544,574	4632	*	16	−0.18	−0.10	*CTB-50L17.14, LRG1, SEMA6B*
chr22	46,449,430	46,451,518	2089	*	18	−0.27	−0.12	*RP6-109B7.5, RP6-109B7.3, FLJ27365, C22orf26*
chr1	42,383,598	42,385,941	2344	*	16	0.33	0.11	*HIVEP3*

Table 3
DMRs uniquely associated with "mild" AGS phenotypes.

Chromosome	Start	End	width	strand	Number of CpGs	maxdiff	meandiff	Genes included in the DMR
chr11	312,518	317,932	5415	*	29	0.23	0.11	*IFITM2, IFITM1*
chr6	31,539,539	31,541,461	1923	*	19	0.18	0.10	*LTA*
chr10	129,533,731	129,537,990	4260	*	22	0.43	0.11	*FOXI2, AL391005.1*
chr17	46,678,719	46,681,635	2917	*	17	0.26	0.12	*HOXB-AS3, HOXB3, HOXB6*
chr6	31,650,735	31,651,676	942	*	20	−0.19	−0.10	*LY6G5C*
chr6	30,038,254	30,039,801	1548	*	32	0.37	0.13	*RNF39*

Table 4
DMRs uniquely associated with "severe" AGS phenotypes.

Chromosome	Start	End	width	strand	Number of CpGs	maxdiff	meandiff	Genes included in the DMR
chr17	79,004,850	79,007,529	2680	*	16	−0.23	−0.13	*BAIAP2-AS1*
chr17	3,704,471	3,708,018	3548	*	15	−0.30	−0.14	*ITGAE, CTD-3195I5.5*
chr13	114,828,264	114,831,550	3287	*	15	−0.29	−0.13	*RASA3*
chr11	67,048,673	67,053,929	5257	*	18	−0.26	−0.12	*ADRBK1*
chr19	850,975	854,522	3548	*	15	−0.24	−0.13	*ELANE*
chr8	144,652,862	144,656,997	4136	*	22	−0.23	−0.10	*RP11-661A12.9, MROH6, NAPRT1*
chr16	4,101,611	4,105,170	3560	*	16	−0.25	−0.12	*ADCY9*
chr14	24,539,335	24,541,377	2043	*	15	−0.25	−0.11	*CPNE6*
chr7	100,463,206	100,465,833	2628	*	17	−0.30	−0.12	*SLC12A9, TRIP6*
chr4	40,191,785	40,195,318	3534	*	18	0.21	0.10	*RHOH*
chr17	46,679,135	46,681,635	2501	*	16	0.24	0.12	*HOXB-AS3, HOXB3, HOXB6*

mutations had been described in AGS [48], may be an attempt of the gene regulation machinery to control pathologic activation of type I IFN pathways by upregulating ADAR expression. Patients with "mild" phenotypes had DMPs located in the promoter region of genes involved in DNA damage and repair mechanisms, including *ATM*, a protein kinase with a key role in DNA damage responses (DDRs). Its canonical activation depends on double-strand breaks (DSBs) and the Mre11-Rad50-Nbs1 (MRN) complex [49] or oxidative stress [50], and was linked to metabolic stress, more precisely to the inhibition of glycolysis [51]. Furthermore, *RAD50* associated with "mild" AGS, orchestrates the DDR response in DSBs, replication fork (RF) collapse, dysfunction of telomeres, and viral invasion [52]. In addition, the *LIG4* gene, also characterized by DMPs, encodes for ligase IV which is part of the non-homologous end-joining mechanism, required for DNA double-stranded break repair, preventing replication fork stalling [53]. Mutations in *RNASEH2B* block the replication fork, thereby contributing to genome instability and extensive DNA damage [54,55]. ATM plays a critical role in limiting DNA damage in *RNASEH2B*-deficient astrocytes, and its inhibition results in increased γH2AX foci (the phosphorylated version of histone H2AX and a marker of DNA damage [56]) and ISG expression [57]. Thus, the DMPs identified here may protect from DNA damage in AGS, resulting in a "milder" phenotype of the disease.

Subsequently, KEGG and GO analyses identified the same general signalling pathways in both "mild" and "severe" AGS phenotypes. Thus, it seems that a shared inflammatory "background" characterized by immune system activation and inflammation may be amplified by the involvement of additional molecular mechanisms in some patients with "severe" AGS. Indeed, considering pathway analyses, "severe" AGS patients exhibited differential DNA methylation in genes involved in developmental processes including embryonic organ, forebrain, and renal system development. Though not detectable on the mRNA level using qPCR, among the genes differentially methylated in "severe" AGS was *ADAMTS9*, a disintegrin and metalloproteinase involved in proteoglycan cleavage and gastrulation [58]. Its expression is induced by inflammatory cytokines [59], suggested as a methylation-based biomarker in osteoarthritis [60]. Another hypomethylated gene in "severe" AGS was the GTPase *RAB34* that regulates phagolysosome formation, thereby priming of $CD8^+$ T cell responses against pathogens [61], and ciliogenesis [62]. Ciliary defects have been linked with a variety of neurological disorders, including cerebellar and brain anomalies [63], highlighting the role and link of these two genes to the neurological symptoms observed in patients with a "severe" AGS phenotype.

In line with altered DNA methylation, differential mRNA expression was observed between controls and AGS patients. Increased mRNA expression was not closely mirrored by reduced DNA methylation in all cases. The ISGs *IFI44* and *RSAD2*, both included in the type I IFN signature proposed by Rice et al. [25] and the here suggested "reduced" IFN signature, exhibit reduced DNA methylation (in their promoter region) alongside increased gene expression. Also, in *RAB34*, *SH2D1B, RAD50* and *ATM*, DNA methylation and mRNA expression were diametric. At *SMG6*, increased DNA methylation in the 1st intron associated with increased mRNA expression, and at *LIG4*, reduced DNA methylation of the 1st intron associated with increased mRNA expression. In both cases, altered methylation does not affect previously reported regulatory regions or coding elements. While no experimental data are available in the literature for these genes, altered methylation may affect recruitment of suppressors or activators of transcription [64]. Notably, in *LIG4*, only regions from 2nd exon and 3′ of it are translated into protein [65]. Increased DNA methylation at *TERF2* affected the 6th exon. This may affect transcription efficacy of the region, which may affect gene expression, but likely has less impact on gene expression when compared to alterations to regulatory elements [66,67]. Lastly,

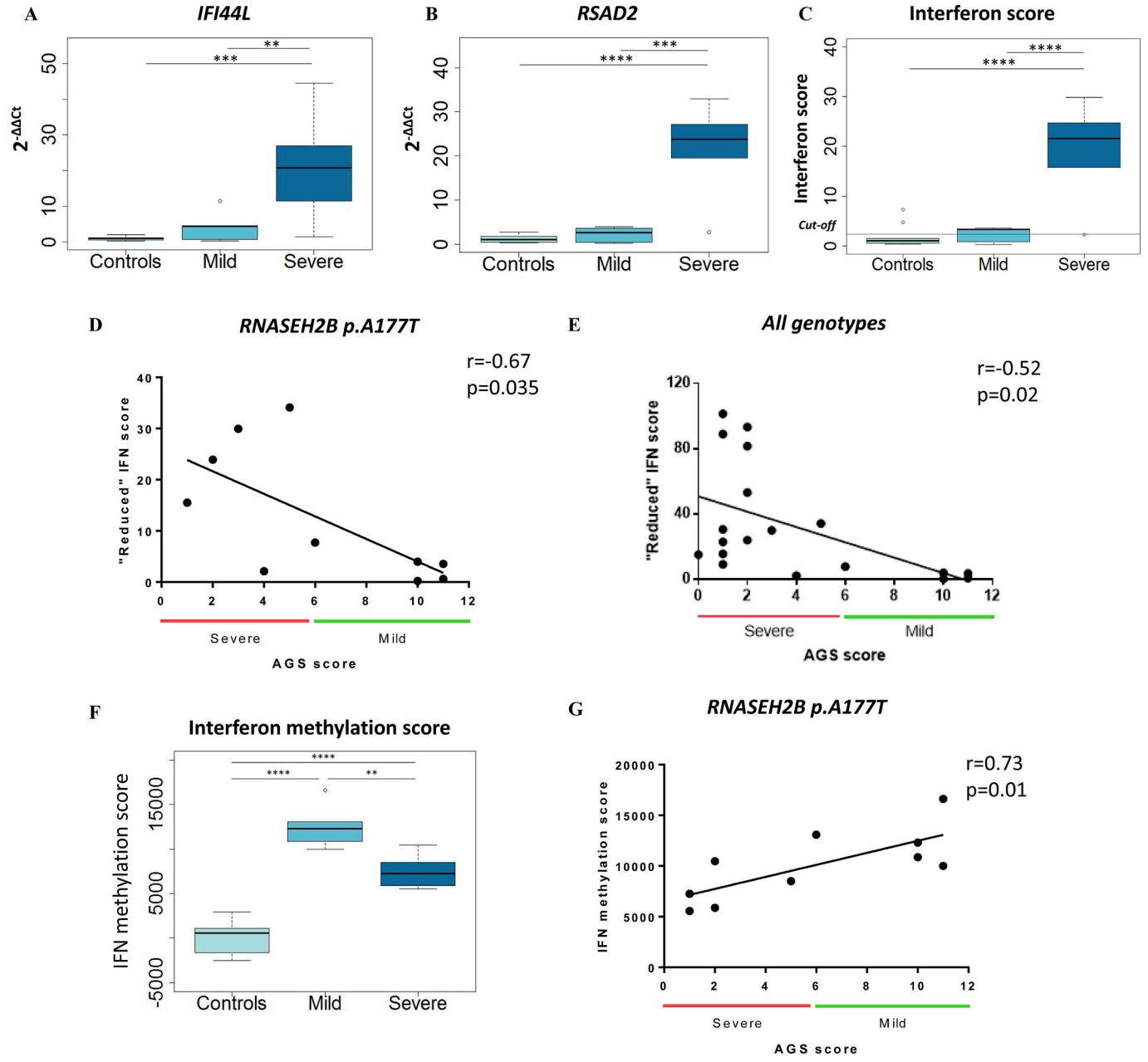

Fig. 4. ISG expression and interferon scores in relation to AGS phenotypes. (A, B) Relative quantification (RQ) of interferon-stimulated genes (ISGs) *IFI44L* and *RSAD2*. (C) IFN scores were calculated as the median of the RQ of the two ISGs in patients and healthy controls. The line represents the cut-off value (2.46) determined according to the method reported by Rice et al. (25). Results are reported as mean ± standard deviation. Data were analyzed with Tukey's tests (* $p < 0.05$; ** $p < 0.01$; *** $p < 0.001$; ****$p < 0.0001$). (D) Correlation analysis between IFN scores and AGS scores ("mild" versus "severe" AGS) in patients with the *RNASEH2B* p.A177T mutation. After assessing Gaussian distribution, Pearson tests were used to test correlation. Patients were considered to have a classic severe form of AGS when the score is included between 0 and 5 (red line), mild when the score is between 6 and 12 (green line). *$p < 0.05$ (E) Correlation analysis between IFN scores and AGS scores of AGS patients with additional genotypes. *$p < 0.05$ (F) IFN methylation score calculated in patients and healthy control according to the method reported by Björk et al. (27). Results are reported as mean ± standard deviation. Data were analyzed with Tukey's test (** $p < 0.01$; ****$p < 0.0001$). (G) Correlation between IFN methylation scores and AGS clinical scores in patients with *RNASEH2B* p.A177T mutations. *$p < 0.05$. (For interpretation of the references to colour in this figure legend, the reader is referred to the web version of this article.)

though *ADAMTS9* expression was not detected on the mRNA level in ex vivo isolated PBMCs, reduced DNA methylation in patients with AGS suggests increased ability for gene expression. Indeed, as mentioned above, DNA methylation is only one of the players involved gene regulation that regulates chromatin accessibility to the transcriptional complex [68]. Lastly, for all seeming discrepancies between methylation and gene expression, it must be considered that gene expression can be affected by activation status of immune cells, the transcription factor micro-environment, most of which can be affected by sample handling and experimental conditions [69,70].

Considering DMRs containing a minimum of 15 CpGs, 4 DMRs common between "mild" and "severe" AGS were identified proximal to 10 genes, including the transcription factor HIVEP3 (Human Immunodeficiency Virus Type I Enhancer-Binding Protein). HIVEP3 regulates inflammatory pathways and may have a critical role in the female predilection of SLE [71]. It is involved in cognitive function and pain modulation [72], and polymorphisms are associated with Parkinson's disease [73–76]. Another gene of interest in the vicinity of these DMRs,

SEMA6B, is hypermethylated in AGS. SEMA6B plays a role in axon guidance and neurodevelopment [77–79]. A stop mutation in *SEMA6B* was reported in a patient with global developmental delay, progressive ataxia, epilepsy and disabling positive and negative truncal myoclonus [80], and truncating variants affecting the last exon have been linked with progressive myoclonic epilepsy [81]. Furthermore, the Leucine Rich Alpha-2-Glycoprotein 1 (*LRG1*), an acute phase protein [82] elevated in the cerebrospinal fluid (CSF) during neuroinflammation and bacterial meningitis [83], was hypermethylated in AGS patients. Lastly, a hypermethylated DMR affecting the histidine ammonia-lyase (HAL) encoding gene was observed. This enzyme is involved in histidine metabolism and functional impairment was linked with oxidative stress in rheumatoid arthritis and chronic kidney disease [84], and neurodevelopmental delay [85]. Six DMRs uniquely associated with "mild" AGS and affected 10 genes. Enriched GO terms were related to responses to IFN-α/−β, and regulation of viral entry and cell cycle. IFN-β release in AGS patients is the consequence of an accumulation of undigested endogenous nucleic acids that mimic a viral infection [5]. Thus, the affected ISGs *IFITM1* and *IFITM2* encode for the interferon induced transmembrane proteins 1 and 2, and their altered methylation and expression were reported also in other autoimmune diseases, including Sjögren's syndrome and SLE [86,87]. The *LTA* gene, encoding for lymphotoxin-α, belongs to the TNF superfamily and is involved in multiple sclerosis (MS), Alzheimer's disease and cerebrovascular diseases. In MS, up-regulation of LTA in the CSF, CNS plaques and active brain lesions may cause inflammatory exacerbation, promote demyelination, and impede remyelination [88]. The transcription factors HOXB3 and HOXB6 are part of the developmental regulatory system and confer specific positional identities to cells along the anterior-posterior axis [89,90]. HOXB3 plays a role in glioblastoma development by promoting proliferation and cell invasion of glioma cells [91]. Roubroeks et al. identified 12 hypermethylated regions in *HOXB6* that associated with Alzheimer's disease [92]. The *RNF39* gene, encoding for the transcription factor RNF39 (Ring Finger Protein 39), is located in the MHC class 1 region on chromosome 6. It is associated with early synaptic plasticity and has been linked with MS [93]. In Japanese populations, *RNF39* polymorphisms are associated with Behçet's disease, an autoinflammatory vasculitis with neurological involvement [94]. Lastly, hypomethylation of this gene was identified in $CD4^+$ T cells from SLE [95] and MS patients [93].

A total of 11 DMRs specifically associated with "severe" AGS affected 17 genes. Several genes, including *ITGAE, ELANE, RHOH*, *ADRBK1* and *RASA3* have previously been linked to immunological pathways. *ITGAE*, encodes for the Integrin Subunit Alpha E, also known as CD103, a marker of memory T cells. It contributes to the development of airway inflammation in asthma [96], participates in the development of allergic contact hypersensitivity [97], and the induction of cutaneous inflammatory disorders [98]. In inflammatory MS lesions, $CD8^+$ T cells exhibited reduced expression of surface molecules involved in leukocyte egress from inflamed tissues and increased CD103 expression [99,100]. A demethylated region affecting the *ELANE* gene was observed exclusively in "severe" AGS. The *ELANE* gene encodes for neutrophil specific elastase that plays a role in granulocyte differentiation [101,102]; its deficiency causes neutropenia, a common finding in AGS [4]. The *RHOH* gene, that was hypomethylated in "severe" AGS, encodes for the atypical Rho GTPase which is predominantly expressed by hematopoietic cells. Increased expression allows bypassing TCR β-selection, a key step in T cell development [103]. Its dysregulated expression has been linked to SLE, primary immunodeficiencies and psoriasis [104]. The *ADRBK1* gene is hypermethylated in "severe AGS" and encodes the G protein-coupled receptor kinase 2. In microglial cells, GRK2 regulates TLR3-, TLR4-, and TLR-9-mediated inflammatory signalling [105] and inflammation-induced neurodegeneration [106]. The RAS P21 protein activator 3, encoded by the *RASA3* gene, plays a role in erythropoiesis and megakaryopoiesis. It is involved in cell cycle progression and maintenance of ROS levels during terminal erythroid differentiation [107]. Its deficiency affects thrombopoiesis and associates with severe thrombocytopenia [108], a symptom associated with AGS [1,4]. RASA3 plays a critical role in T cell migration, homeostasis, and function [109]. In MS, RASA3 is involved in the generation and (dys-)regulation of pathogenic Th17 cells [110]. "Severe" AGS patients exhibited hypermethylation of RASA3, which may contribute to reduced gene expression and increased generation of pathogenic Th17 cells. While the role of Th17 cells in AGS has not been investigated yet, these effector T cells are closely linked to the pathophysiology of SLE [111]. Lastly, 4 "severe" AGS associated DMRs affected *NAPRT1, ADCY9, CPNE6, SLC12A9*, all involved in cell metabolism. Extracellular NAPRT (eNAPRT) levels are increased in acute inflammatory diseases, contributing to the activation of macrophages [112]. Loss-of-function mutations associated with schizophrenia, and partial loss of *NAPRT1* function alters brain development in zebrafish [113]. Niacin (the substrate of NAPRT1) bioavailability is crucial for neuronal survival and function in humans; its deficiency is a pathogenic factor for neurological deficits and dementia, neuronal injury and psychiatric disorders [114]. The *ADCY9* gene encodes for adenyl cyclase type 9 that hydrolyses ATP to produce the second messenger cyclic AMP. It is the most abundantly expressed adenylate cyclase in the brain [115]. Cyclic AMP has a central role in signalling pathways associated with the pathogenesis of immune-mediated diseases, including SLE [116]. The *CPNE6* gene encodes for Copine-6, a calcium sensor expressed in the postnatal brain [117] and is hypermethylated in "severe" AGS patients. Copine-6 regulates spontaneous neurotransmission within central synapses and its overexpression leads to a decrease in the frequency of spontaneous miniature post-synaptic currents. Downregulation of copine-6 increases the frequency of these currents [118]. Abnormal expression in the brain may play a role in epilepsy [119] and may contribute to structural and synaptic plasticity, learning and memory [117,120]. *SLC12A9* and *TRPI6* are in the same hypermethylated region. *SLC12A9* encodes for an electroneutral cation-chloride cotransporter of currently unknown function [121]. The Thyroid Hormone Receptor Interactor 6 (TRIP6) is an adaptor protein that interacts with a variety of proteins controlling cellular processes including transcription, motility, cytoskeletal remodelling, activation of NF-κB and the expression of TNF-α and IL-6 [122], brain ciliogenesis [123] and neurodevelopment [124–126].

Taken together DMPs and DMRs identified in AGS relate to genes involved in inflammatory responses, immunodeficiency, and neuronal development or neuropathology. This suggests that altered DNA methylation may not only serve as a marker of disease severity, but also represent future therapeutic targets to alter disease outcomes. Interferon expression (*IFI44L*, *RSAD2*) and methylation scores correlate with AGS disease severity. However, correlation of gene expression scores is relatively weak when compared to DNA methylation scores. These differences may be caused by DNA methylation being more robust that mRNA expression, especially in relation to environmental factors affecting the patient (stress, temperature, infections, etc.) but also the biospecimen collected [69,70].

While this study delivers promising results suggesting DNA methylation as future tool for activity assessment, outcome prediction and, potentially, even therapeutic target, it has limitations. The relatively small number of AGS patient in the cohort should, however, be seen in the context of the rarity of this pathology. Furthermore, while matched for sex and ethnicity, patient samples were not age matched. Due to legislation in Italy, healthy individuals were adults. We corrected for this in silico during data analysis. Bulk PBMCs, rather than single immune cell subsets, were chosen because of small blood volumes available from young children and the associated challenge of achieving high enough DNA concentrations for sequencing. For the future, we are planning studies in single immune cell subpopulations. Lastly, data is from a single centre cohort (national reference centre in Italy). Further work is needed to confirm findings in larger unrelated and multi-ethnic cohorts, and may result in tools to predict neurodevelopmental outcomes, monitor responses to treatment, disease activity and progression.

5. Conclusions

DNA methylation patterns are altered in peripheral immune cells from AGS patients. Differential DNA methylation may contribute to inflammation, disease phenotypes and severity in AGS patients with the *RNASEH2B* p.A177T mutation. This is reflected by increased ISG expression in patients with "severe" as compared to "mild" phenotypes. Molecular interferon scores based on gene expression or DNA methylation, including *IFI44L* and *RSAD2* expression, associate with "severe" disease and may serve as predictor of disease courses and inform individualized care. Results require confirmation in larger independent AGS patient cohorts, also including patients with additional disease-causing mutations.

Funding

This work was supported by the Italian Ministry of Health grant RC 2020-2023 and by NIH-funded grants (U01NS106845-01A1).

Authors' contributions

Conception and design of the study: J. Garau, AC, CH; acquisition of data SO, EF, J. Galli, SG, OP, CC, CH; analysis of data: J. Garau, AC, FD; interpretation of data: J. Garau, AC, CV, CH; drafting the article J. Garau, AC, CV, CH; critically revision for important intellectual content: SO, EF, J. Galli, SG, OP, CC, CH; final approval of the version to be submitted: all authors.

Declaration of Competing Interest

No financial conflicts of interest were reported by the authors.

Data availability

The data presented in the study will be deposited in the GEO repository.

Acknowledgments

We would like to thank the International AGS Association (IAGSA) for its support and commitment to our project.

Appendix A. Supplementary data

Supplementary data to this article can be found online at https://doi.org/10.1016/j.clim.2023.109299.

References

[1] S. Orcesi, R. La Piana, E. Fazzi, Aicardi-Goutieres syndrome, Br. Med. Bull. 89 (2009) 183–201, https://doi.org/10.1093/bmb/ldn049.
[2] G. Ramantani, J. Kohlhase, C. Hertzberg, et al., Expanding the phenotypic spectrum of lupus erythematosus in Aicardi-Goutières syndrome, Arthritis Rheum. 62 (2010) 1469–1477, https://doi.org/10.1002/art.27367.
[3] M.A. Lee-Kirsch, C. Wolf, C. Günther, Aicardi-Goutières syndrome: a model disease for systemic *autoimmunity*, Clin. Exp. Immunol. 175 (2014) 17–24, https://doi.org/10.1111/cei.12160.
[4] L.A. Adang, F. Gavazzi, R. D'Aiello, et al., Hematologic abnormalities in Aicardi Goutières syndrome, Mol. Genet. Metab. 136 (2022) 324–329, https://doi.org/10.1016/j.ymgme.2022.06.003.
[5] Y.J. Crow, N. Manel, Aicardi-Goutières syndrome and the type I interferonopathies, Nat. Rev. Immunol. 15 (2015) 429–440, https://doi.org/10.1038/nri3850.
[6] C. Uggenti, A. Lepelley, M. Depp, et al., cGAS-mediated induction of type I interferon due to inborn errors of histone pre-mRNA processing, Nat. Genet. 52 (2021) 1364–1372, https://doi.org/10.1038/s41588-020-00737-3.
[7] Y.J. Crow, D.S. Chase, J. Lowenstein Schmidt, et al., Characterization of human disease phenotypes associated with mutations in TREX1, RNASEH2A, RNASEH2B, RNASEH2C, SAMHD1, ADAR, and IFIH1, Am. J. Med. Genet. Part A 167A (2015) 296–312, https://doi.org/10.1002/ajmg.a.36887.
[8] J. Garau, V. Cavallera, M. Valente, et al., Molecular genetics and interferon signature in the Italian Aicardi Goutières syndrome cohort: report of 12 new cases and literature review, J. Clin. Med. 8 (2019) 750, https://doi.org/10.3390/jcm8050750.
[9] C. Günther, B. Kind, M.A. Reijns, et al., Defective removal of ribonucleotides from DNA promotes systemic autoimmunity, J. Clin. Invest. 125 (2015) 413–424, https://doi.org/10.1172/JCI78001.
[10] L.A. Adang, F. Gavazzi, M. De Simone, et al., Developmental outcomes of Aicardi Goutières syndrome, J. Child Neurol. 35 (2020) 7–16, https://doi.org/10.1177/0883073819870944.
[11] L.A. Adang, F. Gavazzi, A.F. Jawad, et al., Development of a neurologic severity scale for Aicardi Goutières syndrome, Mol. Genet. Metab. 130 (2020) 153–160, https://doi.org/10.1016/j.ymgme.2020.03.008.
[12] C.M. Hedrich, K. Mäbert, T. Rauen, G.C. Tsokos, DNA methylation in systemic lupus erythematosus, Epigenomics 9 (2017) 505–525, https://doi.org/10.2217/epi-2016-0096.
[13] A. Charras, J. Garau, S.R. Hofmann, et al., DNA methylation patterns in CD8+ T cells discern psoriasis from psoriatic arthritis and correlate with cutaneous disease activity, Front. Cell Dev. Biol. 9 (2021) 746145, https://doi.org/10.3389/fcell.2021.746145.
[14] S.Y. Lin, S.C. Hsieh, Y.C. Lin, et al., A whole genome methylation analysis of systemic lupus erythematosus: hypomethylation of the IL10 and IL1R2 promoters is associated with disease activity, Genes Immun. 13 (2012) 214–220, https://doi.org/10.1038/gene.2011.74.
[15] Y.W. Lim, L.A. Sanz, X. Xu, S.R. Hartono, F. Chédin, Genome-wide DNA hypomethylation and RNA:DNA hybrid accumulation in Aicardi-Goutières syndrome, eLife 4 (2015), https://doi.org/10.7554/eLife.08007 e08007.
[16] R. Palisano, P. Rosenbaum, S. Walter, D. Russell, E. Wood, B. Galuppi, Development and reliability of a system to classify gross motor function in children with cerebral palsy, Dev. Med. Child Neurol. 39 (1997) 214–223, https://doi.org/10.1111/j.1469-8749.1997.tb07414.x.
[17] A.C. Eliasson, L. Krumlinde-Sundholm, B. Rösblad, E. Beckung, M. Arner, A. M. Ohrvall, P. Rosenbaum, The manual ability classification system (MACS) for children with cerebral palsy: scale development and evidence of validity and reliability, Dev. Med. Child Neurol. 48 (2006) 549–554, https://doi.org/10.1017/S0012162206001162.
[18] M.J. Hidecker, N. Paneth, P.L. Rosenbaum, et al., Developing and validating the communication function classification system for individuals with cerebral palsy, Dev. Med. Child Neurol. 53 (2011) 704–710, https://doi.org/10.1111/j.1469-8749.2011.03996.x.
[19] M.J. Aryee, A.E. Jaffe, H. Corrada-Bravo, C. Ladd-Acosta, A.P. Feinberg, K. D. Hansen, R.A. Irizarry, Minfi: a flexible and comprehensive Bioconductor package for the analysis of Infinium DNA methylation microarrays, Bioinformatics 30 (2014) 1363–1369, https://doi.org/10.1093/bioinformatics/btu049.
[20] Y. Tian, T.J. Morris, A.P. Webster, Z. Yang, S. Beck, A. Feber, A.E. Teschendorff, ChAMP: updated methylation analysis pipeline for Illumina BeadChips, Bioinformatics 33 (2017) 3982–3984, https://doi.org/10.1093/bioinformatics/btx513.
[21] W.E. Johnson, C. Li, A. Rabinovic, Adjusting batch effects in microarray expression data using empirical Bayes methods, Biostatistics 8 (2007) 118–127, https://doi.org/10.1093/biostatistics/kxj037.
[22] M.E. Ritchie, B. Phipson, D. Wu, et al., Limma powers differential expression analyses for RNA-sequencing and microarray studies, Nucleic Acids Res. 43 (2015) e47, https://doi.org/10.1093/nar/gkv007.
[23] T.J. Peters, M.J. Buckley, A.L. Statham, et al., De novo identification of differentially methylated regions in the human genome, Epigenetics Chromatin 8 (2015) 6, https://doi.org/10.1186/1756-8935-8-6.
[24] G. Yu, L.G. Wang, Y. Han, Q.Y. He, clusterProfiler: an R package for comparing biological themes among gene clusters, OMICS 16 (2012) 284–287, https://doi.org/10.1089/omi.2011.0118.
[25] G.I. Rice, G.M. Forte, M. Szynkiewicz, et al., Assessment of interferon-related biomarkers in Aicardi-Goutières syndrome associated with mutations in TREX1, RNASEH2A, RNASEH2B, RNASEH2C, SAMHD1, and ADAR: a case-control study, Lancet Neurol. 12 (2013) 1159–1169, https://doi.org/10.1016/S1474-4422(13)70258-8.
[26] K.J. Livak, T.D. Schmittgen, Analysis of relative gene expression data using real-time quantitative PCR and the 2(-Delta Delta C(T)) method, Methods (San Diego, Calif.) 25 (2001) 402–408, https://doi.org/10.1006/meth.2001.1262.
[27] I. Rusinova, S. Forster, S. Yu, et al., Interferome v2.0: an updated database of annotated interferon-regulated genes, Nucleic Acids Res. 41 (2013) D1040–D1046, https://doi.org/10.1093/nar/gks1215.
[28] A. Björk, E. Richardsdotter Andersson, J. Imgenberg-Kreuz, et al., Protein and DNA methylation-based scores as surrogate markers for interferon system activation in patients with primary Sjögren's syndrome, RMD Open 6 (2020), https://doi.org/10.1136/rmdopen-2019-000995 e000995.
[29] M.M. Suzuki, A. Bird, DNA methylation landscapes: provocative insights from epigenomics, Nat. Rev. Genet. 9 (2008) 465–476, https://doi.org/10.1038/nrg2341.
[30] A.E.A. Surace, C.M. Hedrich, The role of epigenetics in autoimmune/inflammatory disease, Front. Immunol. 10 (2019) 1525, https://doi.org/10.3389/fimmu.2019.01525.
[31] R. Vento-Tormo, D. Álvarez-Errico, A. Garcia-Gomez, et al., DNA demethylation of inflammasome-associated genes is enhanced in patients with cryopyrin-associated periodic syndromes, J. Allergy Clin. Immunol. 139 (2017) 202–211.e6, https://doi.org/10.1016/j.jaci.2016.05.016.

[32] E.G. Toraño, M.G. García, J.L. Fernández-Morera, P. Niño-García, A.F. Fernández, The impact of external factors on the epigenome: in utero and over lifetime, Biomed. Res. Int. (2016) 2568635, https://doi.org/10.1155/2016/2568635.
[33] J.M.P. Woo, C.G. Parks, S. Jacobsen, K.H. Costenbader, S. Bernatsky, The role of environmental exposures and gene-environment interactions in the etiology of systemic lupus erythematous, J. Intern. Med. 291 (2022) 755–778, https://doi.org/10.1111/joim.13448.
[34] B.M. Javierre, A.F. Fernandez, J. Richter, et al., Changes in the pattern of DNA methylation associate with twin discordance in systemic lupus erythematosus, Genome Res. 20 (2010) 170–179, https://doi.org/10.1101/gr.100289.109.
[35] E. Ballestar, A.H. Sawalha, Q. Lu, Clinical value of DNA methylation markers in autoimmune rheumatic diseases, Nat. Rev. Rheumatol. 16 (2020) 514–524, https://doi.org/10.1038/s41584-020-0470-9.
[36] X. Liu, C. Gorzelanny, S.W. Schneider, Platelets in skin autoimmune diseases, Front. Immunol. 10 (2019) 1453, https://doi.org/10.3389/fimmu.2019.01453.
[37] G. Passacquale, P. Vamadevan, L. Pereira, C. Hamid, V. Corrigall, A. Ferro, Monocyte-platelet interaction induces a pro-inflammatory phenotype in circulating monocytes, PLoS One 6 (2011), https://doi.org/10.1371/journal.pone.0025595 e25595.
[38] Y. Chen, H. Zhong, Y. Zhao, X. Luo, W. Gao, Role of platelet biomarkers in inflammatory response, Biomark Res. 8 (2020) 28, https://doi.org/10.1186/s40364-020-00207-2.
[39] J.D. van Buul, P.L. Hordijk, Signaling in leukocyte transendothelial migration, Arterioscler. Thromb. Vasc. Biol. 24 (2004) 824–833, https://doi.org/10.1161/01.ATV.0000122854.76267.5c.
[40] A. Izzotti, A. Pulliero, S. Orcesi, et al., Interferon-related transcriptome alterations in the cerebrospinal fluid cells of Aicardi-Goutières patients, Brain Pathol. 19 (2009) 650–660, https://doi.org/10.1111/j.1750-3639.2008.00229.x.
[41] C.J. Ulff-Møller, F. Asmar, Y. Liu, et al., Twin DNA methylation profiling reveals flare-dependent interferon signature and B cell promoter hypermethylation in systemic lupus erythematosus, Arthritis Rheumatol. 70 (2018) 878–890, https://doi.org/10.1002/art.40422.
[42] D.M. Absher, X. Li, L.L. Waite, et al., Genome-wide DNA methylation analysis of systemic lupus erythematosus reveals persistent hypomethylation of interferon genes and compositional changes to CD4+ T-cell populations, PLoS Genet. 9 (2013), https://doi.org/10.1371/journal.pgen.1003678 e1003678.
[43] J. Imgenberg-Kreuz, J.C. Almlöf, D. Leonard, et al., Shared and unique patterns of DNA methylation in systemic lupus erythematosus and primary Sjögren's syndrome, Front. Immunol. 10 (2019) 1686, https://doi.org/10.3389/fimmu.2019.01686.
[44] J. Imgenberg-Kreuz, J.K. Sandling, J.C. Almlöf, et al., Genome-wide DNA methylation analysis in multiple tissues in primary Sjögren's syndrome reveals regulatory effects at interferon-induced genes, Ann. Rheum. Dis. 75 (2016) 2029–2036, https://doi.org/10.1136/annrheumdis-2015-208659.
[45] J. Imgenberg-Kreuz, J. Carlsson Almlöf, D. Leonard, et al., DNA methylation mapping identifies gene regulatory effects in patients with systemic lupus erythematosus, Ann. Rheum. Dis. 77 (2018) 736–743, https://doi.org/10.1136/annrheumdis-2017-212379.
[46] F.A.H. Cooles, J.D. Isaacs, The interferon gene signature as a clinically relevant biomarker in autoimmune rheumatic disease, Lancet Rheumatol. 4 (1) (2022) e61–e72, https://doi.org/10.1016/S2665-9913(21)00254-X.
[47] M.M. Mukaka, Statistics corner: a guide to appropriate use of correlation coefficient in medical research, Malawi Med. J. J. Med. Assoc. Malawi 24 (2012) 69–71.
[48] G.I. Rice, P.R. Kasher, G.M. Forte, N.M. Mannion, S.M. Greenwood, M. Szynkiewicz, J.E. Dickerson, Mutations in ADAR1 cause Aicardi-Goutières syndrome associated with a type I interferon signature, Nat. Genet. 44 (2012) 1243–1248, https://doi.org/10.1038/ng.2414.
[49] J.H. Lee, T.T. Paull, ATM activation by DNA double-strand breaks through the Mre11-Rad50-Nbs1 complex, Science 308 (2005) 551–554, https://doi.org/10.1126/science.1108297.
[50] Z. Guo, S. Kozlov, M.F. Lavin, M.D. Person, T.T. Paull, ATM activation by oxidative stress, Science 330 (2010) 517–521, https://doi.org/10.1126/science.1192912.
[51] A.J. Yeo, K.L. Chong, M. Gatei, et al., Impaired endoplasmic reticulum-mitochondrial signaling in ataxia-telangiectasia, iScience 24 (2020) 101972, https://doi.org/10.1016/j.isci.2020.101972.
[52] A. Syed, J.A. Tainer, The MRE11-RAD50-NBS1 complex conducts the orchestration of damage signaling and outcomes to stress in DNA replication and repair, Annu. Rev. Biochem. 87 (2018) 263–294, https://doi.org/10.1146/annurev-biochem-062917-012415.
[53] R.R. Joshi, S.I. Ali, A.K. Ashley, DNA ligase IV prevents replication fork stalling and promotes cellular proliferation in triple negative breast cancer, J. Nucleic Acids 2019 (2019) 9170341, https://doi.org/10.1155/2019/9170341.
[54] S. Pizzi, S. Sertic, S. Orcesi, et al., Reduction of hRNase H2 activity in Aicardi-Goutières syndrome cells leads to replication stress and genome instability, Hum. Mol. Genet. 24 (2015) 649–658, https://doi.org/10.1093/hmg/ddu485.
[55] K. Bartsch, K. Knittler, C. Borowski, et al., Absence of RNase H2 triggers generation of immunogenic micronuclei removed by autophagy, Hum. Mol. Genet. 26 (2017) 3960–3972, https://doi.org/10.1093/hmg/ddx283.
[56] A. Sharma, K. Singh, A. Almasan, Histone H2AX phosphorylation: a marker for DNA damage, Methods Mol. Biol. 920 (2012) 613–626, https://doi.org/10.1007/978-1-61779-998-3_40.
[57] A.M.S. Giordano, M. Luciani, F. Gatto, et al., DNA damage contributes to neurotoxic inflammation in Aicardi-Goutières syndrome astrocytes, J. Exp. Med. 219 (2022), https://doi.org/10.1084/jem.20211121 e20211121.
[58] R.P. Somerville, J.M. Longpre, K.A. Jungers, et al., Characterization of ADAMTS-9 and ADAMTS-20 as a distinct ADAMTS subfamily related to Caenorhabditis elegans GON-1, J. Biol. Chem. 278 (2003) 9503–9513, https://doi.org/10.1074/jbc.M211009200.
[59] S. Nandadasa, C.M. Kraft, L.W. Wang, et al., Secreted metalloproteases ADAMTS9 and ADAMTS20 have a non-canonical role in ciliary vesicle growth during ciliogenesis, Nat. Commun. 10 (2019) 953, https://doi.org/10.1038/s41467-019-08520-7.
[60] T. Ohtsuki, A. Shinaoka, K. Kumagishi-Shinaoka, et al., Mechanical strain attenuates cytokine-induced ADAMTS9 expression via transient receptor potential vanilloid type 1, Exp. Cell Res. 383 (2019) 111556, https://doi.org/10.1016/j.yexcr.2019.111556.
[61] A. Alloatti, F. Kotsias, A.M. Pauwels, et al., Toll-like receptor 4 engagement on dendritic cells restrains phago-lysosome fusion and promotes cross-presentation of antigens, Immunity 43 (2015) 1087–1100, https://doi.org/10.1016/j.immuni.2015.11.006.
[62] M.W. Stuck, W.M. Chong, J.C. Liao, G.J. Pazour, Rab34 is necessary for early stages of intracellular ciliogenesis, Curr. Biol. 31 (2021) 2887–2894.e4, https://doi.org/10.1016/j.cub.2021.04.018.
[63] S.M. Ware, M.G. Aygun, F. Hildebrandt, Spectrum of clinical diseases caused by disorders of primary cilia, Proc. Am. Thorac. Soc. 8 (2011) 444–450, https://doi.org/10.1513/pats.201103-025SD.
[64] O. Bell, V.K. Tiwari, N.H. Thomä, D. Schübeler, Determinants and dynamics of genome accessibility, Nat. Rev. Genet. 12 (2011) 554–564, https://doi.org/10.1038/nrg3017.
[65] D. Anastasiadi, A. Esteve-Codina, F. Piferrer, Consistent inverse correlation between DNA methylation of the first intron and gene expression across tissues and species, Epigenetics Chromatin 11 (2018) 37, https://doi.org/10.1186/s13072-018-0205-1.
[66] J.A. Cain, B. Montibus, R.J. Oakey, Intragenic CpG Islands and their impact on gene regulation, Front. Cell Dev. Biol. 10 (2022) 832348, https://doi.org/10.3389/fcell.2022.832348.
[67] A. Angeloni, O. Bogdanovic, Enhancer DNA methylation: implications for gene regulation, Essays Biochem. 63 (2019) 707–715, https://doi.org/10.1042/EBC20190030.
[68] E.R. Gibney, C.M. Nolan, Epigenetics and gene expression, Heredity 105 (2010) 4–13, https://doi.org/10.1038/hdy.2010.54.
[69] Y. Li, X. Pan, M.L. Roberts, et al., Stability of global methylation profiles of whole blood and extracted DNA under different storage durations and conditions, Epigenomics 10 (2018) 797–811, https://doi.org/10.2217/epi-2018-0025.
[70] A. Paziewska, M. Dabrowska, K. Goryca, et al., DNA methylation status is more reliable than gene expression at detecting cancer in prostate biopsy, Br. J. Cancer 111 (2014) 781–789, https://doi.org/10.1038/bjc.2014.337.
[71] N.A. Young, A.K. Friedman, B. Kaffenberger, et al., Novel estrogen target gene ZAS3 is overexpressed in systemic lupus erythematosus, Mol. Immunol. 54 (2013) 23–31, https://doi.org/10.1016/j.molimm.2012.10.026.
[72] L.C. Wu, V.M. Goettl, F. Madiai, K.V. Hackshaw, S.R. Hussain, Reciprocal regulation of nuclear factor kappa B and its inhibitor ZAS3 after peripheral nerve injury, BMC Neurosci. 7 (2006) 4, https://doi.org/10.1186/1471-2202-7-4.
[73] S.A. Oliveira, Y.J. Li, M.A. Noureddine, S. Zuchner, X. Qin, M.A. Pericak-Vance, J. M. Vance, Identification of risk and age-at-onset genes on chromosome 1p in Parkinson disease, Am. J. Hum. Genet. 77 (2005) 252–264, https://doi.org/10.1086/432588.
[74] J.Y. Wan, K.L. Edwards, C.M. Hutter, et al., Association mapping of the PARK10 region for Parkinson's disease susceptibility genes, Parkinsonism Relat. Disord. 20 (2014) 93–98, https://doi.org/10.1016/j.parkreldis.2013.10.001.
[75] K. Kolarikova, R. Vodicka, R. Vrtel, J. Stellmachova, M. Prochazka, K. Mensikova, P. Kanovsky, Whole exome sequencing study in isolated south-eastern Moravia (Czechia) population indicates heterogenous genetic background for parkinsonism development, Front. Neurosci. 16 (2022), 817713, https://doi.org/10.3389/fnins.2022.817713.
[76] Y.J. Li, J. Deng, G.M. Mayhew, J.W. Grimsley, X. Huo, J.M. Vance, Investigation of the PARK10 gene in Parkinson disease, Ann. Hum. Genet. 71 (2007) 639–647, https://doi.org/10.1111/j.1469-1809.2007.00353.x.
[77] L.T. Alto, J.R. Terman, Semaphorins and their signaling mechanisms, Methods Mol. Biol. 1493 (2017) 1–25, https://doi.org/10.1007/978-1-4939-6448-2_1.
[78] S.M. Kanth, S. Gairhe, P. Torabi-Parizi, The role of semaphorins and their receptors in innate immune responses and clinical diseases of acute inflammation, Front. Immunol. 12 (2021) 672441, https://doi.org/10.3389/fimmu.2021.672441.
[79] A. Cordovado, M. Schaettin, M. Jeanne, et al., SEMA6B variants cause intellectual disability and alter dendritic spine density and axon guidance, Hum. Mol. Genet. 31 (2022) 3325–3340, https://doi.org/10.1093/hmg/ddac114.
[80] R. Herzog, Y. Hellenbroich, N. Brüggemann, et al., Zonisamide-responsive myoclonus in SEMA6B-associated progressive myoclonic epilepsy, Ann. Clin. Transl. Neurol. 8 (2021) 1524–1527, https://doi.org/10.1002/acn3.51403.
[81] K. Hamanaka, E. Imagawa, E. Koshimizu, et al., De novo truncating variants in the last exon of SEMA6B cause progressive myoclonic epilepsy, Am. J. Hum. Genet. 106 (2020) 549–558, https://doi.org/10.1016/j.ajhg.2020.02.011.
[82] R. Codina, A. Vanasse, A. Kelekar, V. Vezys, R. Jemmerson, Cytochrome c-induced lymphocyte death from the outside in: inhibition by serum leucine-rich alpha-2-glycoprotein-1, Apoptosis 15 (2010) 139–152, https://doi.org/10.1007/s10495-009-0412-0.
[83] K. Talukder, R. Prasad, A. Abhinay, A. Singh, R. Srivastava, O.P. Mishra, T. B. Singh, Cerebrospinal fluid leucine-rich alpha-2 glycoprotein (LRG) levels in

children with acute bacterial meningitis, Indian J. Pediatr. 89 (2022) 192–194, https://doi.org/10.1007/s12098-021-03972-6.
[84] B. Yu, A.H. Li, D. Muzny, et al., Association of Rare Loss-of-Function Alleles in HAL, serum histidine: levels and incident coronary heart disease, Circ. Cardiovasc. Genet. 8 (2015) 351–355, https://doi.org/10.1161/CIRCGENETICS.114.000697.
[85] M.E. Brosnan, J.T. Brosnan, Histidine metabolism and function, J. Nutr. 150 (2020) 2570S–2575S, https://doi.org/10.1093/jn/nxaa079.
[86] M. Teruel, G. Barturen, M. Martínez-Bueno, et al., Integrative epigenomics in Sjögren's syndrome reveals novel pathways and a strong interaction between the HLA, autoantibodies and the interferon signature, Sci. Rep. 11 (2021) 23292, https://doi.org/10.1038/s41598-021-01324-0.
[87] C.D. Scharer, E.L. Blalock, T. Mi, et al., Epigenetic programming underpins B cell dysfunction in human SLE, Nat. Immunol. 20 (2019) 1071–1082, https://doi.org/10.1038/s41590-019-0419-9.
[88] M. Mallya, R.D. Campbell, B. Aguado, Characterization of the five novel Ly-6 superfamily members encoded in the MHC, and detection of cells expressing their potential ligands, Protein Sci. 15 (2006) 2244–2256, https://doi.org/10.1110/ps.062242606.
[89] L.F. Wockner, C.P. Morris, E.P. Noble, B.R. Lawford, V.L. Whitehall, R.M. Young, J. Voisey, Brain-specific epigenetic markers of schizophrenia, Transl. Psychiatry 5 (2015), https://doi.org/10.1038/tp.2015.177 e680.
[90] I.A. Lindhout, T.E. Murray, C.M. Richards, A. Klegeris, Potential neurotoxic activity of diverse molecules released by microglia, Neurochem. Int. 148 (2021) 105117, https://doi.org/10.1016/j.neuint.2021.105117.
[91] I. Kreicberga, A. Junga, M. Pilmane, Investigation of HoxB3 and growth factors expression in placentas of various gestational ages, J. Dev. Biol. 10 (2021) 2, https://doi.org/10.3390/jdb10010002.
[92] L.G. Kömüves, W.F. Shen, A. Kwong, et al., Changes in HOXB6 homeodomain protein structure and localization during human epidermal development and differentiation, Dev. Dyn. 218 (2000) 636–647, https://doi.org/10.1002/1097-0177(2000)9999:9999<::AID-DVDY1014>3.0.CO;2-I.
[93] K. Xu, C. Qiu, H. Pei, M.A. Mehmood, H. Wang, L. Li, Q. Xia, Homeobox B3 promotes tumor cell proliferation and invasion in glioblastoma, Oncol. Lett. 15 (2018) 3712–3718, https://doi.org/10.3892/ol.2018.7750.
[94] J.A.Y. Roubroeks, A.R. Smith, R.G. Smith, et al., An epigenome-wide association study of Alzheimer's disease blood highlights robust DNA hypermethylation in the HOXB6 gene, Neurobiol. Aging 95 (2020) 26–45, https://doi.org/10.1016/j.neurobiolaging.2020.06.023.
[95] V.E. Maltby, R.A. Lea, K.A. Sanders, N. White, M.C. Benton, R.J. Scott, J. Lechner-Scott, Differential methylation at MHC in CD4+ T cells is associated with multiple sclerosis independently of HLA-DRB1, Clin. Epigenetics 9 (2017) 71, https://doi.org/10.1186/s13148-017-0371-1.
[96] R. Kurata, H. Nakaoka, A. Tajima, et al., TRIM39 and RNF39 are associated with Behçet's disease independently of HLA-B*51 and -A*26, Biochem. Biophys. Res. Commun. 401 (2010) 533–537, https://doi.org/10.1016/j.bbrc.2010.09.088.
[97] P. Renauer, P. Coit, M.A. Jeffries, J.T. Merrill, W.J. McCune, K. Maksimowicz-McKinnon, A.H. Sawalha, DNA methylation patterns in naïve CD4+ T cells identify epigenetic susceptibility loci for malar rash and discoid rash in systemic lupus erythematosus, Lupus Sci. Med. 2 (2015), https://doi.org/10.1136/lupus-2015-000101 e000101.
[98] E. Bernatchez, M.J. Gold, A. Langlois, et al., Pulmonary CD103 expression regulates airway inflammation in asthma, Am. J. Physiol. Lung Cell. Mol. Physiol. 308 (2015) L816–L826, https://doi.org/10.1152/ajplung.00319.2014.
[99] A. Braun, N. Dewert, F. Brunnert, et al., Integrin αE(CD103) is involved in regulatory T-cell function in allergic contact hypersensitivity, J. Invest. Dermatol. 135 (2015) 2982–2991, https://doi.org/10.1038/jid.2015.287.
[100] M.P. Schön, M. Schön, H.B. Warren, J.P. Donohue, C.M. Parker, Cutaneous inflammatory disorder in integrin alphaE (CD103)-deficient mice, J. Immunol. 165 (2000) 6583–6589.
[101] J. Machado-Santos, E. Saji, A.R. Tröscher, et al., The compartmentalized inflammatory response in the multiple sclerosis brain is composed of tissue-resident CD8+ T lymphocytes and B cells, Brain 141 (2018) 2066–2082, https://doi.org/10.1093/brain/awy151.
[102] N.L. Fransen, C.C. Hsiao, M. van der Poel, et al., Tissue-resident memory T cells invade the brain parenchyma in multiple sclerosis white matter lesions, Brain 143 (2020) 1714–1730, https://doi.org/10.1093/brain/awaa117.
[103] P. Mistry, S. Nakabo, L. O'Neil, et al., Transcriptomic, epigenetic, and functional analyses implicate neutrophil diversity in the pathogenesis of systemic lupus erythematosus, Proc. Natl. Acad. Sci. U. S. A. 116 (2019) 25222–25228, https://doi.org/10.1073/pnas.1908576116.
[104] B. Garg, H.M. Mehta, B. Wang, R. Kamel, M.S. Horwitz, S.J. Corey, Inducible expression of a disease-associated ELANE mutation impairs granulocytic differentiation, without eliciting an unfolded protein response, J. Biol. Chem. 295 (2020) 7492–7500, https://doi.org/10.1074/jbc.RA120.012366.
[105] N. Tamehiro, H. Oda, M. Shirai, H. Suzuki, Overexpression of RhoH permits to bypass the pre-TCR checkpoint, PLoS One 10 (2015), https://doi.org/10.1371/journal.pone.0131047 e0131047.
[106] A.M. Ahmad Mokhtar, I.F. Hashim, M. Mohd Zaini Makhtar, N.H. Salikin, S. Amin-Nordin, The role of RhoH in TCR signalling and its involvement in diseases, Cells 10 (2021) 950, https://doi.org/10.3390/cells10040950.
[107] S. Palikhe, W. Ohashi, T. Sakamoto, et al., Regulatory role of GRK2 in the TLR signaling-mediated iNOS induction pathway in microglial cells, Front. Pharmacol. 10 (2019) 59, https://doi.org/10.3389/fphar.2019.00059.
[108] V. Degos, S. Peineau, C. Nijboer, et al., G protein-coupled receptor kinase 2 and group I metabotropic glutamate receptors mediate inflammation-induced sensitization to excitotoxic neurodegeneration, Ann. Neurol. 73 (2013) 667–678, https://doi.org/10.1002/ana.23868.
[109] E.S. Hartman, E.C. Brindley, J. Papoin, S.L. Ciciotte, Y. Zhao, L.L. Peters, L. Blanc, Increased reactive oxygen species and cell cycle defects contribute to anemia in the RASA3 mutant mouse model scat, Front. Physiol. 9 (2018) 689, https://doi.org/10.3389/fphys.2018.00689.
[110] R.H. Lee, D. Ghalloussi, G.L. Harousseau, et al., Rasa3 deficiency minimally affects thrombopoiesis but promotes severe thrombocytopenia due to integrin-dependent platelet clearance, JCI Insight 7 (2022), https://doi.org/10.1172/jci.insight.155676 e155676.
[111] K.H. Johansen, D.P. Golec, B. Huang, et al., A CRISPR screen targeting PI3K effectors identifies RASA3 as a negative regulator of LFA-1-mediated adhesion in T cells, Sci. Signal. 15 (2022), https://doi.org/10.1126/scisignal.abl9169 eabl9169.
[112] N. Celarain, J. Tomas-Roig, Changes in deoxyribonucleic acid methylation contribute to the pathophysiology of multiple sclerosis, Front. Genet. 10 (2019) 1138, https://doi.org/10.3389/fgene.2019.01138.
[113] J.C. Crispín, C.M. Hedrich, G.C. Tsokos, Gene-function studies in systemic lupus erythematosus, Nat. Rev. Rheumatol. 9 (2013) 476–484, https://doi.org/10.1038/nrrheum.2013.78.
[114] V. Audrito, V.G. Messana, S. Deaglio, NAMPT and NAPRT: two metabolic enzymes with key roles in inflammation, Front. Oncol. 10 (2020) 358, https://doi.org/10.3389/fonc.2020.00358.
[115] S. Periyasamy, S. John, R. Padmavati, et al., Association of schizophrenia risk with Disordered Niacin Metabolism in an Indian genome-wide association study, JAMA Psychiatry 76 (2019) 1026–1034, https://doi.org/10.1001/jamapsychiatry.2019.1335.
[116] V. Gasperi, M. Sibilano, I. Savini, M.V. Catani, Niacin in the central nervous system: an update of biological aspects and clinical applications, Int. J. Mol. Sci. 20 (2019) 974, https://doi.org/10.3390/ijms20040974.
[117] K. Devasani, Y. Yao, Expression and functions of adenylyl cyclases in the CNS, Fluids Barriers CNS 19 (2022) 23, https://doi.org/10.1186/s12987-022-00322-2.
[118] H.M. Teixeira, N.M. Alcantara-Neves, M. Barreto, C.A. Figueiredo, R.S. Costa, Adenylyl cyclase type 9 gene polymorphisms are associated with asthma and allergy in Brazilian children, Mol. Immunol. 82 (2017) 137–145, https://doi.org/10.1016/j.molimm.2017.01.001.
[119] J.R. Reinhard, A. Kriz, M. Galic, N. Angliker, M. Rajalu, K.E. Vogt, M.A. Ruegg, The calcium sensor Copine-6 regulates spine structural plasticity and learning and memory, Nat. Commun. 7 (2016) 11613, https://doi.org/10.1038/ncomms11613.
[120] P. Liu, M. Khvotchev, Y.C. Li, N.L. Chanaday, E.T. Kavalali, Copine-6 binds to SNAREs and selectively suppresses spontaneous neurotransmission, J. Neurosci. 38 (2018) 5888–5899, https://doi.org/10.1523/JNEUROSCI.0461-18.2018.
[121] B. Zhu, J. Zha, Y. Long, X. Hu, G. Chen, X. Wang, Increased expression of copine VI in patients with refractory epilepsy and a rat model, J. Neurol. Sci. 360 (2016) 30–36, https://doi.org/10.1016/j.jns.2015.11.041.
[122] K. Burk, B. Ramachandran, S. Ahmed, et al., Regulation of dendritic spine morphology in hippocampal neurons by Copine-6, Cereb. Cortex 28 (2018) 1087–1104, https://doi.org/10.1093/cercor/bhx009.
[123] K.B. Gagnon, E. Delpire, Physiology of SLC12 transporters: lessons from inherited human genetic mutations and genetically engineered mouse knockouts, Am. J. Physiol. Cell Physiol. 304 (2013) C693–C714, https://doi.org/10.1152/ajpcell.00350.2012.
[124] Y. Yang, X.M. Li, J.R. Wang, et al., TRIP6 promotes inflammatory damage via the activation of TRAF6 signaling in a murine model of DSS-induced colitis, J. Inflamm. (Lond.) 19 (2022) 1, https://doi.org/10.1186/s12950-021-00298-0.
[125] S. Shukla, R. Haenold, P. Urbánek, et al., TRIP6 functions in brain ciliogenesis, Nat. Commun. 12 (2021) 5887, https://doi.org/10.1038/s41467-021-26057-6.
[126] Y.H. Youn, Y.G. Han, Primary cilia in brain development and diseases, Am. J. Pathol. 188 (2018) 11–22, https://doi.org/10.1016/j.ajpath.2017.08.031.